https://doi.org/10.5194/egusphere-2024-1279
Preprint. Discussion started: 13 May 2024

From the Top: Surface-derived Carbon Fuels Greenhouse Gas Production at Depth in a Neotropical Peatland

Alexandra Hedgpeth[1,2], Alison M. Hoyt[3], Kyle Cavanaugh[1], Karis J. McFarlane[2*], Daniela F. Cusack[1,4,5*]

[1]Geography Department, University of California Los Angeles, Los Angeles, 94143, USA
[2]Lawrence Livermore National Laboratory, Livermore, 94550, USA
[3]Department of Earth System Science, Stanford University, Stanford, 94305, USA
[4] Department of Ecosystem Science & Sustainability, Colorado State University, Fort Collins, 80523, USA
[5]Smithsonian Tropical Research Institute, Balboa, Ancon, Republic of Panama, 0843-03092

★ These authors contributed equally to this work

Correspondence: Alexandra Hedgpeth (hedgpea10@g.ucla.edu)

Abstract.

Tropical peatlands play an important role in global carbon (C) cycling but little is known about factors driving carbon dioxide (CO_2) and methane (CH_4) emissions from these ecosystems, especially production below the surface. This study aimed to identify source material and processes regulating C emissions from deep in a Neotropical peatland on the Caribbean coast of Panama. We hypothesized that: 1) surface derived organic matter transported down the soil profile is the primary C source for respiration products at depth and 2) high lignin content results in hydrogenotrophic methanogenesis as the dominant CH_4 production pathway throughout the profile. We used radiocarbon isotopes to determine whether CO_2 and CH_4 at depth (measured to 2m) are produced from modern substrates or ancient deep peat, and we used stable C isotopes to identify the dominant CH_4 production pathway. Peat organic chemistry was characterized using ^{13}C solid state nuclear magnetic resonance spectroscopy (^{13}C-NMR). We found that deep peat respiration products had radiocarbon signatures that were more similar to surface dissolved organic C (DOC) than deep solid peat. Radiocarbon ages for deep peat ranged from 1200 – 1800 yrBP at the sites measured. These results indicate that surface derived C was the dominant source for gas production at depth in this peatland, likely because of vertical transport of DOC from the surface to depth. Carbohydrates did not vary with depth across these sites, whereas lignin, which was the most abundant compound (55-70% of C), tended to increase with depth. These results suggest that there is no preferential decomposition of carbohydrates, but preferential retention of lignin. Stable isotope signatures of respiration products indicated that hydrogenotrophic rather than acetoclastic methanogenesis was the dominant production pathway of CH_4 throughout the peat profile. These results suggest, even C compounds that are typically considered vulnerable to decomposition (i.e., carbohydrates) are preserved deep in these tropical peats, highlighting the importance of anaerobic, waterlogged conditions for preserving tropical peatland C.

https://doi.org/10.5194/egusphere-2024-1279
Preprint. Discussion started: 13 May 2024

1 Introduction

Climate change is expected to disturb hydrological cycles in the tropics, with changes in rainfall regimes already observed for many tropical regions (Kharin et al. 2007, Feng et al. 2013, Magrin et al. 2014, Duffy et al. 2015, Chadwick et al. 2016, Barkhordarian et al. 2019). Changes in rainfall are of particular relevance to the storage of the 70 – 130 Gt of carbon (C) stored in tropical peatland soils under anaerobic conditions, which could be under threat of rapid mineralization if rainfall declines and aerobic conditions emerge (Girkin et al., 2022; Loisel et al., 2021). Tropical peatlands store the largest pool of vulnerable and irrecoverable C of any ecosystem type, and this pool is sequestered over thousands of years (Goldstein et al., 2020; Noon et al., 2021). Despite their importance, tropical peatlands are logistically challenging environments to work in and are understudied compared to their northern counterparts, making tropical peatlands underrepresented in global C inventories (Ribeiro et al., 2021).

Peatlands sequester C as they build vertically with the oldest deposits at the base and less decomposed younger material accumulating at the surface (Clymo et al., 1998; Ingram, 1987). Despite temperatures ideal for microbial activity, the buildup of organic matter is possible because rates of primary production in the tropics exceed decomposition rates, which are low because peatland water tables are high (Page et al., 2011; Nottingham et al., 2019). Thus, deep peat is comprised of minimally processed plant material from the surface that accumulates due to anaerobic conditions, creating a globally significant buildup of C over time that could be metabolized if conditions became more favorable for decomposition (Hoyos-Santillan et al., 2019; Wilson et al., 2021; Kettridge et al., 2015). However, this age-depth relationship is not as straightforward in the tropics as in northern peatlands, because tropical peatland microtopography shows higher variability due to increased vegetation diversity and size, and forest disturbance can have dramatic effects on peat accumulation patterns (Dommain et al., 2015; Girkin et al., 2019). The dominant vegetation that acts as the stabilizing structure in early peat development, as well as the vegetation that serves as the biological origin of the peat itself, is also different in northern and tropical peatlands, leading to differences in peatland development, organic chemistry, and accumulation patterns between these two regions (United Nations Environment Programme et al., 2008).

Under current conditions, there is considerable variation in C emissions across tropical wetland systems (Fritts, 2022; Farmer et al., 2011), but some relationships have been generally characterized. It is mostly accepted that water table depth (Hoyos-Santillan et al., 2019; Hoyt et al., 2019; Cobb et al., 2017), temperature (Hirano et al., 2009; Girkin et al., 2020), substrate availability, and associated links with the dominant vegetation type (Wright et al., 2013, 2011; Upton et al., 2018), are strong controls on atmospheric emissions from tropical peatlands. Furthermore, surface vegetation plays an important role in the release of C by several processes, including being the biological origin of the peat matrix, which is composed primarily of lignin rich fibrous material in woody tropical peatlands, and determining labile C inputs in the form of decomposing plant tissues or root exudates (Osaki et al., 2021; Girkin et al., 2018b; Lampela et al., 2014). The majority of studies conducted in tropical peatlands have focused on the top 30 cm of the peat column; these depths are not only more accessible and easier to measure, but they are assumed to contribute the majority of emissions (Sjögersten et al., 2011; Jauhiainen et al., 2005;

https://doi.org/10.5194/egusphere-2024-1279
Preprint. Discussion started: 13 May 2024

Dhandapani et al., 2022). However, it is not known if the above drivers are mainly restricted to the surface, or if these processes influence CO_2 and CH_4 production deeper within the peat profile.

In many peatlands, microbial respiration across the soil profile can be supported by multiple C sources, and it is possible to use the radiocarbon signature of C respired from peatlands to partition sources into modern/surface dissolved organic C (DOC) transported down the soil profile, versus older/buried solid C (Chanton et al., 2008; Hoyos-Santillan et al., 2016). Modern DOC, derived from surface vegetation, root exudates, and other recently photosynthesized organic matter, has a signature that is enriched in ^{14}C. The existing peat and DOC from *in situ* decomposition of that deep peat, would have depleted radiocarbon signatures compared to the modern DOC (Girkin et al., 2018b; Wilson et al., 2016).

There have been several studies exploring the source of DOC used by microbes for respiration within peat soils. Most studies were from northern peatlands, and determined that respiration products were intermediate in their radiocarbon activity between newer surface DOC and *in situ* older C in peat (Aravena et al., 1993; Chanton et al., 2008; Charman et al., 1999; Chanton et al., 1995; Elizabeth Corbett et al., 2013; Clymo and Bryant, 2008). Fewer studies have reported that respiration products are more similar to modern DOC radiocarbon signatures, demonstrating dominant use of surface DOC in deep peat gas production (Wilson et al., 2021). There is limited data from tropical peatlands, but two previous studies from the tropics have contrasting results; one shows intermediate respiration products (i.e., produced by mixed sources) in a tropical peatland in Borneo (Hoyt, 2014), and another shows modern, surface-derived inputs are the dominant source in sites across the Pastaza-Marañon basin in Peru (Hoyt et al., 2020). Potential explanations for this variable source contribution in tropical peatlands include differences in hydrology across sites, as well as the difference in dominant vegetation across the tropics. Biological origin can influence the chemistry and bioavailability of both modern DOC inputs and the resulting older peat (Gandois et al., 2014; Dhandapani et al., 2023), which could contribute to the different results reported for these two tropical peatlands with distinct surface vegetation.

Methanogenesis is an important pathway of decomposition in wetland systems. Acetoclastic methanogenesis is associated with acetate fermentation and the production of CH_4 from more relatively labile organic compounds such as in fresh DOC, while hydrogenotrophic methanogenesis is associated with CO_2 reduction and is supported by the decomposition of more complex organic matter, such as that which accumulates at depth (Sugimoto and Wada, 1993; Kotsyurbenko et al., 2004). Metabolically, acetoclastic methanogenesis is more efficient in CH_4 production and generally results in higher rates of CH_4 production compared to hydrogenotrophic methanogenesis (Liebner et al., 2015; Kotsyurbenko et al., 2004). Shifts in CH_4 production pathways between acetoclastic methanogenesis and hydrogenotrophic methanogenesis can occur, as have been seen with depth in northern wetlands (Chanton et al., 2008; Hornibrook et al., 2000; Corbett et al., 2013). Therefore, changes in the availability of labile material throughout the peat profile may play an important role in not only supplying the source for CO_2 and CH_4 production but also dictating how and how much CH_4 is produced (Sun et al., 2012).

This study explored sources of C emissions, CH_4 production pathways, and organic carbon chemistry of peat in three sites in a Neotropical peatland in Panama. Previous work suggested that subsurface peat may contribute substantially to net CO_2 and CH_4 flux from this peatland, but the source of C for these emissions was unclear (Wright et al., 2011). We used a

https://doi.org/10.5194/egusphere-2024-1279
Preprint. Discussion started: 13 May 2024

combination of stable and radioisotope signatures of CO_2 and CH_4, and ^{13}C solid state nuclear magnetic resonance spectroscopy (^{13}C-NMR) characterization of peat soils to identify the sources of the C emitted from subsurface (>30 cm) peat. We hypothesized that: 1) surface-derived DOC is the primary C source for microbial respiration products at depth where peat is more chemically complex, reflecting more advanced decomposition at depth, and 2) hydrogenotrophic methanogenesis is the dominant CH_4 production pathway at depth, resulting from the high lignin content typical of tropical peatlands. We report and discuss radiocarbon analyses of subsurface DOC, CH_4, and CO_2 as well as peat molecular characterization assessed via solid state ^{13}C-NMR spectroscopy in a tropical peatland to address the hypotheses.

2 Methods

2.1 Field Site Description

The Bocas Del Toro Province on the Caribbean coast of Panama is home to an internationally recognized wetland (Ramsar site #611), encompassing the 80 km^2 Changuinola peat deposit, an ombrotrophic domed peatland to the southeast of the Changuinola river (Fig. 1). Located 10 km east from the peatland is the town of Bocas del Toro, Isla Colon, where the average annual rainfall and temperature are 4000 mm and 30°C respectively (Isla Colon, STRI Environmental Monitoring Station). There is continuous rainfall throughout the year with no pronounced dry season, although there are two distinct periods of lower rainfall (February–April and September–October). The water table was consistently at the surface of the peatland throughout the sampling period, but has been reported to fluctuate +20 cm to -0.4 m during high or low rainfall (Hoyos-Santillan, 2014). Mean peat temperature 10 cm below the surface is 25 °C and shows little intra-annual variation (Wright et al., 2011). The oldest deposits in the peatland are in the centre of the dome, are estimated to have been formed 4000–4500 years ago, and are roughly 8 m deep (Phillips et al., 1997).

The Changuinola peat deposit developed from *Raphia taedigera* palm swamp, unlike southeast Asia coastal peatlands that begin as sediment trapping mangrove stands (Anderson and Muller, 1975; Phillips et al., 1997). The vegetation communities that formed the Changuinola peat deposits have shifted spatially over time, reflecting variations in environmental conditions, and resulting in spatial heterogeneities in C inputs across the peatland (Phillips and Bustin, 1996; Cohen et al., 1989). At present, there are seven distinct phasic plant communities that form concentric rings within the peat dome. From the periphery and moving to the interior they are as follows: (i) *Rhizophora mangle* mangrove swamp, (ii) mixed back mangrove swamp, (iii) *Raphia taedigera* palm swamp, (iv) mixed forest swamp, (v) stunted *Campnosperma panamensis* forest swamp, (vi) sawgrass/stunted forest swamp and (vii) *Myrica-Cyrilla* bog-plain (Phillips et al., 1997). Previous work showed that nutrient content in the peat was generally higher near the edge (1200 µg-phosphorus (P)g^{-1}, 27mg-nitrogen (N)g^{-1}) and lower in the interior of the peatland (377 µg-Pg^{-1}, 22mg-Ng^{-1}) (Sjögersten et al., 2011; Troxler, 2007; Troxler et al., 2012).

https://doi.org/10.5194/egusphere-2024-1279
Preprint. Discussion started: 13 May 2024

For this study we selected sites in three of the representative plant communities, with dominant vegetation and nutrient patterns described previously. These include Outer (*Raphia taedigera* palm swamp), Intermediate (mixed forest swamp), and Inner (stunted *Campnosperma panamensis* forest swamp) peatland sites (Fig.1). Previous studies conducted within the Changuinola deposit have reported differences in peat properties, root exudate characteristics, and *ex situ* experimental response in lab studies tied to vegetation community (Upton et al., 2018; Girkin et al., 2018b, 2019; Sjögersten et al., 2011; Wright et al., 2013). Previously reported surface (<30 cm) CO_2 flux rates for the outer and inner sites used here varied from 320-500 mg CO2 m^{-2} hr^{-1} with no significant variation between sites (Wright et al., 2011), and subsurface peat across the vegetation gradient (>30 cm) appeared to have similar carbohydrate to aromatic C ratios following initial phases of decomposition occurring at the surface (Upton et al., 2018).

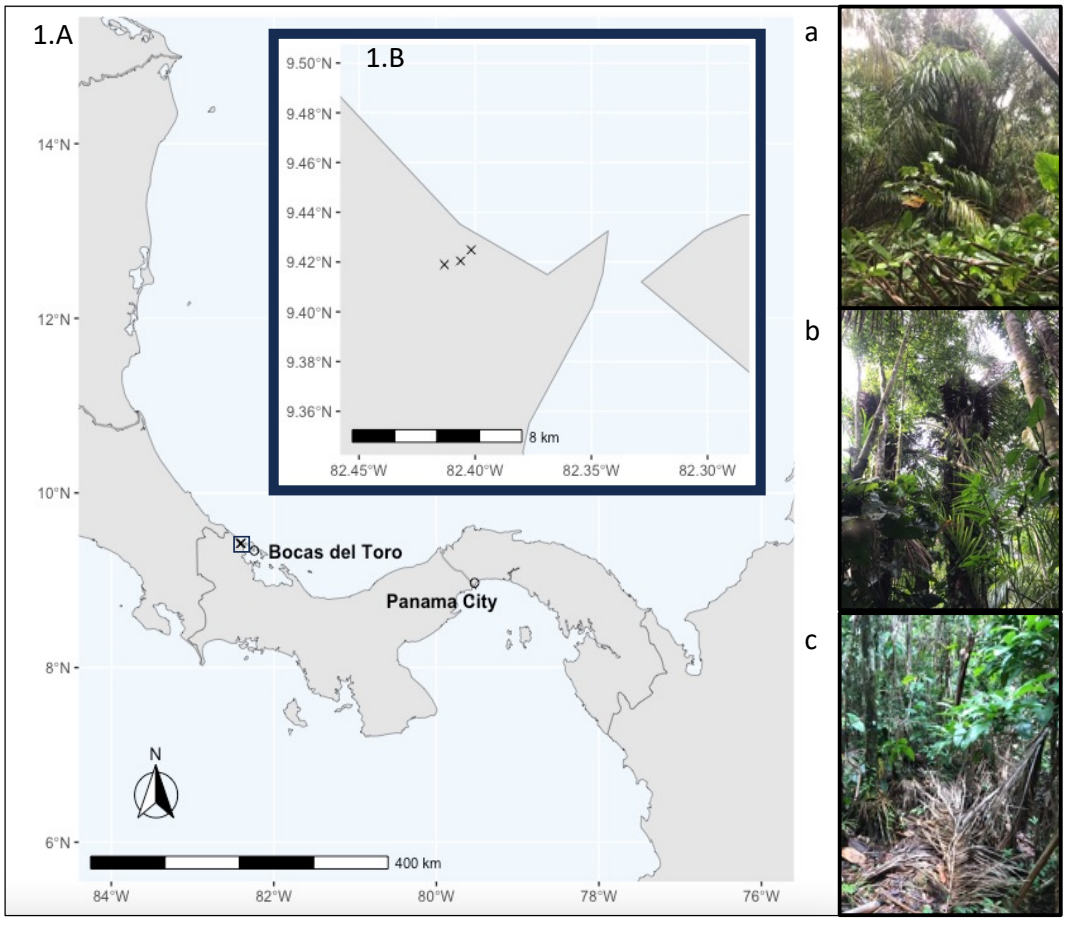

Figure 1: Map of sites included in this study from the Changuinola peat deposit. A. Location of study site identified by square in relation to the city of Bocas Del Toro and Panama City. **B.** Inset showing the location of the sites along the transect. The sites follow a vegetation gradient with a) the outer site closest to the channel *Raphia taedigera* palm swamp b) the intermediate site mixed forest swamp and c) the inner site closest to the centre of the peatland composed of stunted *Campnosperma panamensis* forest swamp. The nutrient gradient decreases from outer site to inner site.

https://doi.org/10.5194/egusphere-2024-1279
Preprint. Discussion started: 13 May 2024

2.2 Sample Collection

Bulk peat, pore water samples, and greenhouse gases (CO_2 and CH_4) were collected in October of 2019. We sampled from 30 cm to basal depths that were identified by a marine clay boundary at the base of the peat, and did not sample surface samples (0–30 cm) that we understand might have stronger surface vegetation influence on peat chemistry compared to deeper layers that are further along in the decomposition process (Barreto and Lindo, 2020). This study aimed to compare bulk peat and pore water components of deep peat with gas produced at the same depth, and for that reason only those deeper samples were collected. Peat cores from were collected using a 5.2 cm diameter and 51 cm long Russian peat corer (Eijkelkamp, Product code 04.09). Bulk peat, pore water samples, and greenhouse gases (CO_2 and CH_4) were collected in October of 2019 from depths of 30 ± 5 and 60 ± 5 cm, as well as 100 ± 5, 200 ± 5, 300 ± 5, and 400 ± 5 cm depending on total peat depth at each site. Porewater was collected using a peristaltic pump with Teflon tubing from 1.25 cm diameter PVC pipe piezometers to measure DOC from the same depths as the peat collection. Porewater was filtered with 45 um particle retention using plastic syringes fitted with stopcocks and filters and deposited into 50 ml falcon tubes for transport. Following collection, peat cores were subsampled to coordinate with gas well depths and sealed in plastic bags to avoid oxidation during transport to the Smithsonian Tropical Research Institute soils lab in Panama City, Panama.

Diffusion gas wells were deployed at the intermediate and outer site at the same depths as pore water and peat collection to ensure robust comparison between the two source materials (bulk peat and DOC) and respiration products. There was insufficient time to include the inner site in gas collection at time of sampling. These diffusion wells consisted of PVC pipe with mesh coverings positioned within the peat to allow water to be sampled from the desired depth without contamination of bulk peat or water pulled from other depths. Water was taken from the desired depth using a peristaltic pump and cycled into a 1L glass container. The headspace within the glass container was allowed to equilibrate over several hours while the water was pumped through the container at a rate of 1.5–1.8 L/min. Air samples from the equilibrated headspace were taken using a syringe fitted with a stopcock and needle and deposited into evacuated 125 ml serum bottles fitted with heavy butyl rubber septa.

2.3 Elemental and Isotopic Analyses

Elemental composition of solid homogenized airdried peat was analysed using an elemental analyser 205 (CHNOS) coupled to an IsoPrime 100 isotope ratio mass spectrometer at the Center for Stable Isotope Biogeochemistry (CSIB) 206 at the University of California, Berkeley. This analysis produced measurements for percent C and N content, ^{13}C, and ^{15}N. The ash content of bulk peat was determined by ignition of aliquots (~1.0 g) at 460°C for 5 hr.

Sample preparation and analysis for ^{14}C was completed at the Center for Accelerator Mass Spectrometry (CAMS) at Lawrence Livermore National Laboratory. To ensure that peat samples were handled appropriately for both biogeochemistry and chronology, following homogenization with a ball and mill grinder we measured two subsamples; one that underwent acid-base-acid (ABA) pre-treatment to remove possible interfering carbonates and modern C derived humic acids, and a second

https://doi.org/10.5194/egusphere-2024-1279
Preprint. Discussion started: 13 May 2024

with no pre-treatment (Norris et al., 2020). Samples were immersed in 1N hydrochloric acid (HCl) to remove carbohydrates. Humic acids were then removed from the sample with 0.25M sodium hydroxide (NaOH) and treated with a 1N HCL immersion before they were rinsed with deionized water until neutral. The pre-treated samples were then placed on a heating block until dried. The two sets of peat samples had identical ^{14}C results and the no pre-treatment values were used in this study (Table A1). The porewater DOC samples were acidified with 1N HCl at 70 ∘C to remove dissolved inorganic C and freeze dried. Both sets of peat samples and the residual DOC were loaded into quartz tubes with excess CuO and combusted at 900∘C to ensure complete combustion to CO_2.

Gas samples for CH_4 and CO_2 were extracted following the protocol outlined by (McNicol et al., 2020). For $^{14}CO_2$ samples, a series of cryogenic traps were used to purify and isolate the CO_2. For $^{14}CH_4$ samples, the mixed composition field samples were cryogenically purified to remove water and CO_2, and the remaining CH_4 was converted to CO_2 by combustion (Petrenko et al., 2008). Resulting CO_2 from samples was split to measure both a $\delta^{13}C$ and ^{14}C. Extracted CO_2 and CH_4 were analysed for ^{14}C and ^{13}C when possible, but some sample masses were too small for both analyses (minimum 20 ug C needed for ^{14}C analysis and for the purpose of this study, we prioritized measurements for ^{14}C). The $\delta^{13}C$ values were analysed at the Stable Isotope Geosciences Facility at Texas 210 A&M University on a Thermo Scientific MAT 253 Dual Inlet Stable Isotope Ratio Mass Spectrometer. To obtain a ^{14}C measurement, the CO_2 was reduced to graphite onto Fe powder in the presence of H2 (Vogel et al., 1984) and analysed on the HVEC 10 MV Model FN Tandem Van de Graaff Accelerator or the NEC 1 MV Pelletron Tandem Accelerator at CAMS (Broek et al., 2021). ^{14}C values are reported as $\Delta^{14}C$ (‰) corrected to the year of measurement (2019) and for mass-dependent fractionation using $\delta^{13}C$ values, and age is reported in years before present (yBP) within two standard deviations using the Libby half-life of 5568 years following the conventions outlined by Stuiver and Polach, 1977. Age-depth models were generated for each site in R v.4.2.2 (The R Foundation for Statistical Computing, 2022) using the "rbacon" package v2.3.9.1. BACON (Bayesian accumulation), is based on Bayesian theory, and simulates the sediment deposition process while accounting for both variable deposition rates and spatial autocorrelation of deposition from one layer to another within the core. Long-term peat accumulation rates were estimated by fitting linear regressions to age-depth model outputs. The calibrated ages showed timing of peat development and accumulation between the three sites, and the conventional radiocarbon values were used to compare and identify the sources of material used to generate CO_2 and CH_4 at depth.

Differences in stable isotopic ($\delta^{13}C$) composition between $\delta^{13}CO_2$ and $\delta^{13}CH_4$ can identify the dominant pathway that produces methane, because hydrogenotrophic methanogenesis fractionate against heavy C isotopes more than acetoclastic methanogenesis (Wilson et al., 2016). Values of this apparent fractionation factor ($\alpha app = [(\delta^{13}CO_2 + 1000)/ (\delta^{13}CH_4 + 1000)]$) that are greater than 1.065 are characteristic of environments dominated by hydrogenotrophic methanogenesis, while values lower than 1.055 are characteristic of environments dominated by acetoclastic methanogenesis (Zhang et al., 2019).

https://doi.org/10.5194/egusphere-2024-1279
Preprint. Discussion started: 13 May 2024

2.4 ^{13}C-NMR Spectroscopy and Mixing Model

Solid State ^{13}C NMR spectra of untreated peat samples were obtained at the Pacific Northwest National Laboratory in Washington state at the Environmental Molecular Science Laboratory facility using cross-polarization under magic angle spinning conditions (CP/MAS) with a Varian Direct Drive NMR spectrometer equipped with a Varian 4-mm probe. These bulk peat samples were free of charcoal. Approximately 30 mg of peat were packed in 4 mm zirconia rotors sealed with Kel-F caps. The CP spectra were acquired after 14k scans with a MAS rate of 14 kHz resulting in no interference from sidebands as they were outside the range of the spectrum, and a ramp-CP contact time on proton of 1 ms and a 1 or 2 s recycle delay depending on the sample with 62.5 kHz tppm proton decoupling (Aliev, 2020). The one-dimensional 1H NMR spectra of all samples were processed and analysed relative to the external standard adamantine. All spectra were corrected against a KBr background, and signals arising from C in the NMR probe and rotor were accounted for by subtracting the spectra of an empty rotor from the sample. Spectra were digitally processed with exponential apodization (100 Hz line broadening with the first point set to 0.50), phase correction, and baseline correction using a Bernstein polynomial fit with Mnova software (v. 14.3.3; Mestrelab Research). Peak areas were integrated within seven chemical shift regions for input to the molecular mixing model corresponding to: alkyl C (0–45 ppm), N-alkyl/methoxyl C (45–60 ppm), O-alkyl C (60–95 ppm), di-O-alkyl (95–110), aromatic C (110–145 ppm), phenolic C (145–165 ppm), and carboxyl C (165–215 ppm).

We used a mixing model which incorporates six components to describe the molecular composition of samples based on ^{13}C NMR outputs (Baldock et al., 2004). This peatland soil has no visual evidence of char, so that component was removed from the model. The five remaining components (carbohydrate, protein, lipid, lignin, and carbonyl) have each been assigned a discrete percent of different regions of the ^{13}C NMR signal intensity based on knowledge of molar elemental contents and C content of terrestrial soil ecosystems. The measured C:N ratio of each sample was used to constrain the protein concentration of each ^{13}C NMR spectrum in the molecular mixing model. The optimisation process of the molecular mixing model compares fits for all five biomolecules to models eliminating one, two, and three components; in all cases the model fit was best when all five components were included in the model (sum of squares of deviation < 6%). The mixing model outputs are available in Table A2.

2.6 Statistics

We assessed our data at two scales: 1) among-site comparisons of the three sites, considering overall differences in peat characteristics and isotopic signatures and 2) peatland-wide patterns in soil profile characteristics and relationships among peat chemistry and isotopic signatures. Relationships between peat physical properties (C and N concentrations, C:N, ^{13}C,^{15}N, and radiocarbon) and the five biomolecules identified with the molecular mixing model were assessed using Pearson correlation analysis. We also conducted separate analyses of the ^{13}C-NMR data using raw data for spectral regions. The three sites were pooled to get peatland scale relationships between the peat physical properties and the five biomolecules versus depth. Due to the limited size of this dataset, the spearman method was used to measure covariance and the coefficients are

https://doi.org/10.5194/egusphere-2024-1279
Preprint. Discussion started: 13 May 2024

reported in the full correlation matrix results, including r^2 values and significance, in supplementary materials (Fig. A3 & A4). We assessed differences among the three sites using Principal Component Analysis (PCA) based on all factors included in the correlation matrices (all peat physical properties, chemistry, and isotopes for each site). Significant trends in biomolecule abundance across depth were identified by linear regression. To identify differences between mean radiocarbon values of the sources and respiration products we utilized two-sample t-tests. Bulk peat and gas products were determined by Welch two-sample t-test to account for lack of homogeneity of variance, and differences between mean radiocarbon values of DOC and gas products were assessed by student two sample t-test. All relationships explored were considered significant at the 0.1 alpha level. Statistical analyses were conducted in R v.4.2.2 (The R Foundation for Statistical Computing, 2022). Reported means in the text are shown with standard errors in parentheses.

3 Results

3.1 Isotopic composition of source material and respiration products

Across all sites and depths, dissolved CH_4 and CO_2 were relatively modern, ^{14}C-enriched relative to peat, and had similar ^{14}C values to DOC, indicating the use of DOC as a preferential substrate over solid peat for microbial respiration (Fig.2). Overall, the respiration products had statistically similar values to the DOC ($t(23)=0.534$ $p= 0.60$) compared to the bulk peat ($t(16)=|8.67|$, $p= <0.05$) (Table S3). The radiocarbon values for the bulk peat are consistent with constant accumulation over time. The calibrated basal ages for outer, intermediate, and inner sites were 1215 ± 35, 1060 ± 30, and 1750 ± 35 yrBP respectively.

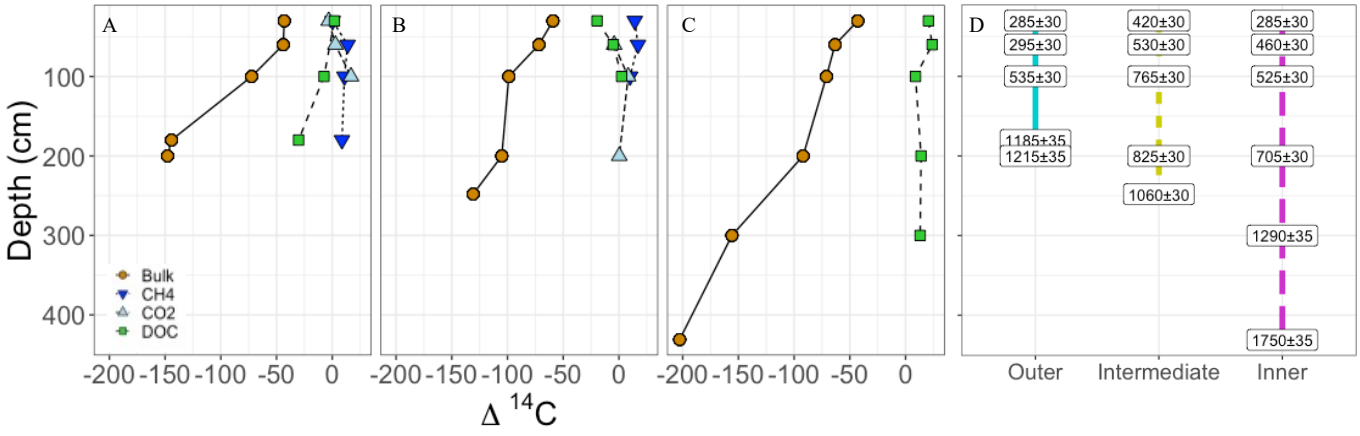

Figure 2. Isotopic composition of respiration products and substrates. Bulk peat, DOC, and respiration products (CH_4 = methane, CO_2 = carbon dioxide) plotted by depth across all three sites; **A)** Outer, **B)** Intermediate and **C)** Inner. Brown circles and solid lines represent bulk peat and green squares with dashed lines represent DOC; these are the two measured sources available for gas production. The gas products are denoted by inverted dark blue triangles and dotted lines for methane, and the light blue triangles and dashed lines for dissolved carbon dioxide. Note the age difference between solid peat and all DOC and gas values; this offset indicates that gas production is driven by modern DOC throughout the peat profile. **D.** Calibrated ages for all bulk peat measured in yBP within two standard deviations for the outer, intermediate, and inner sites denoted by solid blue, dashed yellow, and dashed pink respectively.

https://doi.org/10.5194/egusphere-2024-1279
Preprint. Discussion started: 13 May 2024

3.2 Peat Properties and Chemistry

The percent C across the sites was consistently 40–55% down to basal depths, which had lower C contents and higher ash content, reflecting the influence of underlying mineral sediments (Fig. 3). The negative correlation between both C and N concentrations with depth was not significant, however the negative correlations between ash content and depth ($r(16) = -0.62$, $p \leq 0.1$) and age and depth ($r(16) = -0.93$, $p \leq 0.1$, Fig. 3) were strongly significant (Fig. A3). Bulk peat stable isotopes, $\delta^{13}C$ and $\delta^{15}N$, showed no strong relationship with depth or site. Linear slopes across the age-depth profiles suggested consistent peat accumulation rates across the peatland over time (Fig. 3f). Estimates of long-term peat accumulation rates were calculated using the calibrated ages, and were 0.192 cm yr^{-1}, 0.473 cm yr^{-1}, and 0.275 cm yr^{-1} for the outer, intermediate, and inner sites respectfully.

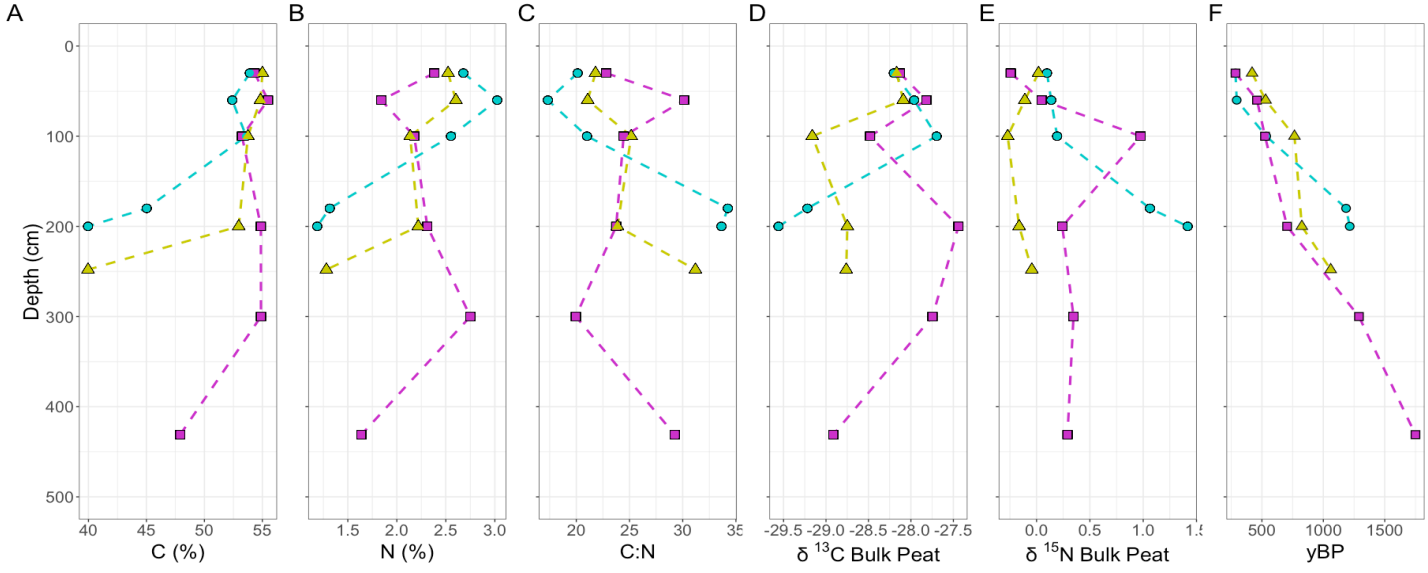

Figure 3. Bulk Peat Properties and Characteristics. Depth profiles for A. percent carbon, B. percent nitrogen, C. the ratio of carbon to nitrogen, D. stable carbon isotope, E. stable nitrogen isotope, and E. calibrated age for layers measured for the three sites. Sites are indicated by colour and shape with blue circles indicating the outer site, yellow triangles the intermediate site, and pink squares the inner site.

Example spectra from surface (30 cm) and deep (basal depths; Outer 200 cm, Intermediate 248 cm, and Inner 431cm) can be seen in Figure 4, and complete spectra datasets can be seen in supplemental material (Fig A1 & A2). The ^{13}C-NMR molecular mixing model results showed that depth was positively correlated with lignin ($r(16) = 0.70$, $p \leq 0.1$) and negatively correlated with lipid abundance ($r(16) = -0.54$, $p \leq 0.1$) (Fig 5.A–C, Fig A4). To further explore patterns in peat chemistry across depth, we pooled the three sites for linear regression. We found significant decreases in lipid abundance ($R^2 = 0.25$, $F(1,14) = 5.88$, $p < 0.029$) and increases in lignin abundance ($R^2 = 0.46$, $F(1,14) = 13.7$, $p < 0.002$) with increasing depth (Fig A6).

Compared to the other four molecular components (protein, lipid, carbonyl, and carbohydrate), lignin was the most abundant biomarker making up an average 64% ± 1.1 of peat organic matter across the sites (Fig 5.D). Carbohydrate was the second most abundant compound and averaged 17% ± 0.2 across the sites. There was almost no carbonyl-C present (all sites

https://doi.org/10.5194/egusphere-2024-1279
Preprint. Discussion started: 13 May 2024

averaged < 2%), except for deep peat at the outer site and 60 and 200 cm layers of the inner site, which had 0.4% ± 0.9 and 2% ± 2 carbonyl-C respectively (Fig 5. A&C). Overall, the organic chemistry of peat was very similar across the sites explored here, and the main patterns that emerged were trends with depth.

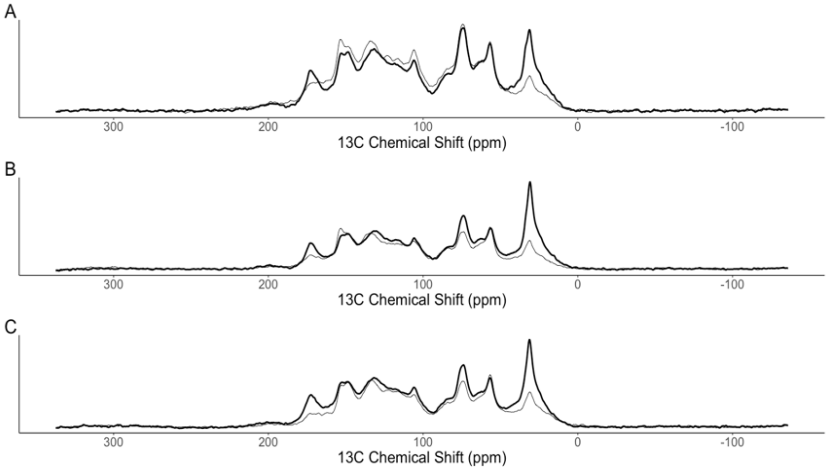

Figure 4. Example 13C NMR spectra. Bulk peat layers sampled from the A. outer, B. intermediate, and C. inner sites showing differences between the shallow (bold) and basal (thin) depths with stacked spectra; the complete spectra dataset can be found in additional data located in supplemental material. Spectra were digitally processed with Mnova software (v. 14.3.3; Mestrelab Research) with exponential apodization (100 Hz line broadening with the first point set to 0.50), phase correction, and baseline correction using a Bernstein polynomial fit.

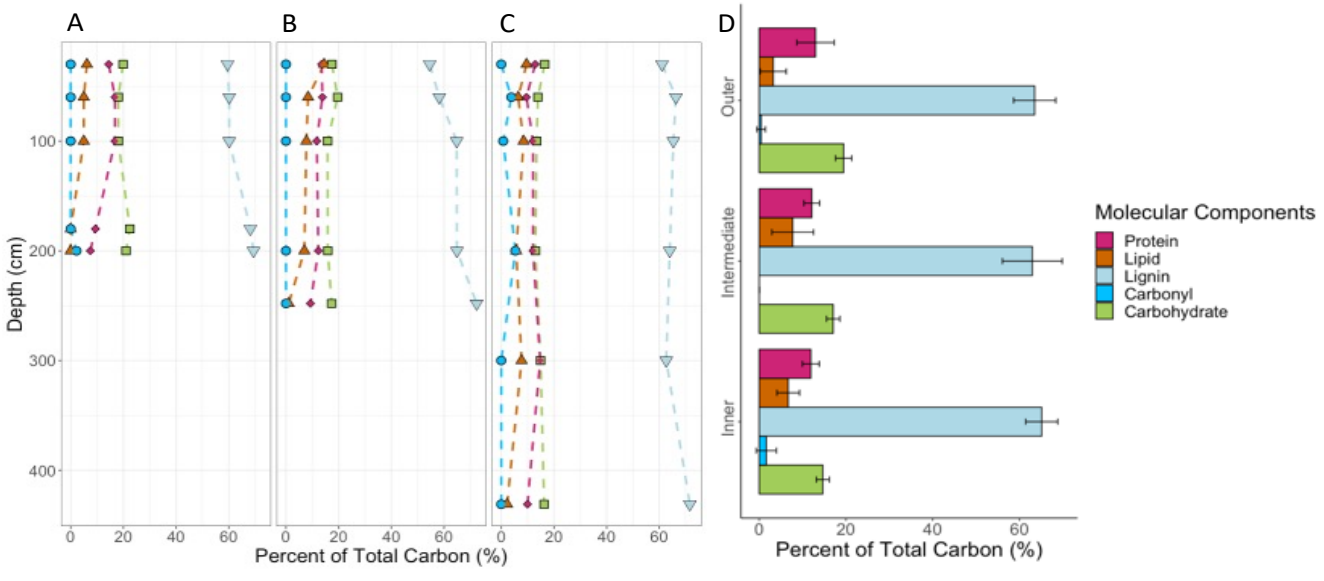

Figure 5. Proportion of total organic C attributed to each molecular component across sites and depths. Mixing model results showing little change in the five molecular components described by the model with depth for the **A)** outer site, **B)** intermediate site, and **C)** inner site. Colours and symbols represent the molecular components with proteins as pink diamonds, lipids as orange triangles, lignin as light blue inverted triangles, carbonyl as blue circles, and carbohydrates as green squares. **D)** Average proportion of total organic C attributed to each molecular component across sites with standard error.

https://doi.org/10.5194/egusphere-2024-1279
Preprint. Discussion started: 13 May 2024

We used PCA to explore differences in peat properties among the three sites. The scores and loadings of the first and second principal components accounted for the majority of variance (74%) with the first principal component accounting for 54.93% (Fig 6). Separation along the first principal component axis showed stratigraphic effects related to depth and peat accumulation over time, with strong separation between the 30 and 60 cm layers versus the underlying peat. The clustering of the 30 and 60 cm peat layers was primarily driven by C and N concentration, age, ash content, and lipid, alkyl-C, and protein contributions to soil organic C (Fig 6, Table A2). By contrast, the second principal component was mainly driven by site differences, with the inner site being relatively more distinct than the outer and intermediate sites while still showing some overlap (Fig 6). This separation appeared to be tied to the small amount of carbonyl present at this site (Fig 6, Table A2, Table A4).

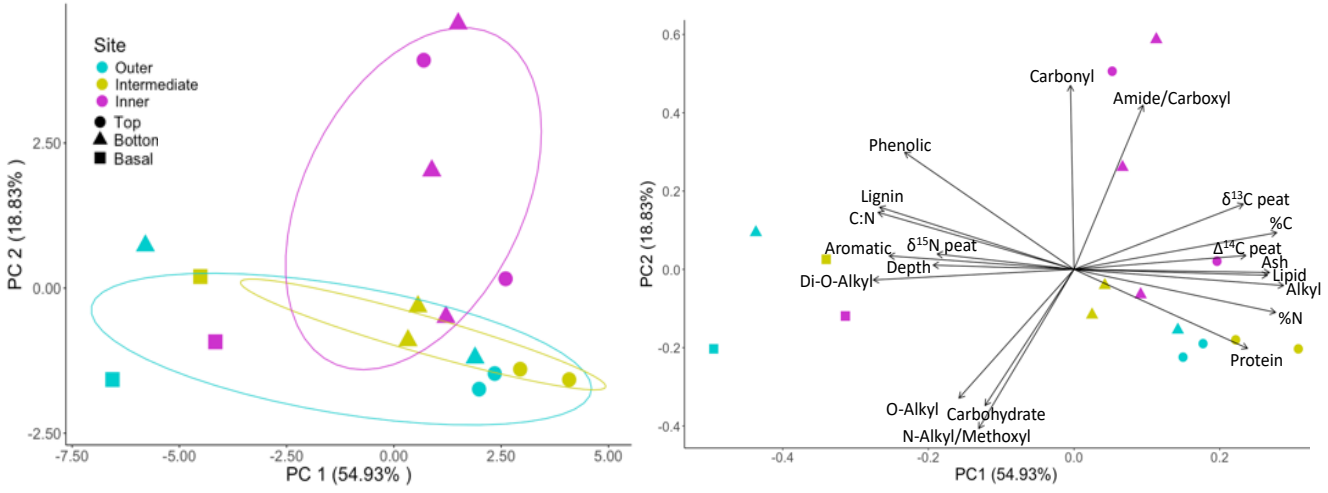

Figure 6. Scores and loadings from the PCA for all peat properties and chemistry and depth for the outer (blue), intermediate (yellow), and inner (pink) sites. Depths have been indicated by shape with the top (30-60 cm) as circles, the bottom (>1 m) as triangles, and the three basal depths as squares (basal depths; Outer 200 cm, Intermediate 248 cm, and Inner 431cm). Combined PC1 and PC2 account for 74% of variance.

https://doi.org/10.5194/egusphere-2024-1279
Preprint. Discussion started: 13 May 2024

3.3 Using $\delta^{13}C$ to identify CH_4 Production Pathway

The α_{app} values overlap between the outer and intermediate sites and averaged 1.078 (+/- 0.003) (Fig. 7). These data demonstrate no shift in α_{app} with depth throughout the peat profile. The α_{app} is consistent with hydrogenotrophic methanogenesis being the dominant production pathway across all depths measured at the outer and intermediate sites.

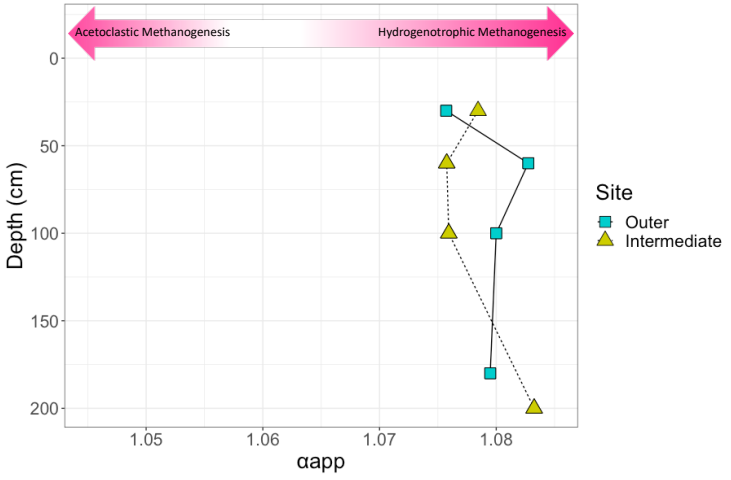

Figure 7. Differences in stable C isotopic composition between DIC and CH_4. Calculated estimates of apparent fractionation factor (αapp) across depth for gas collected from the outer (blue squares) and intermediate (green triangles) sites. The samples from the inner site did not have sufficient amounts of C for this analysis. Note the x-axis shows little variation in αapp between sites and soil layers; values of αapp higher than 1.065 is usually characteristic of environments dominated by hydrogenotrophic methanogenesis, while a value lower than 1.055 is characteristic of an environment dominated by acetoclastic methanogenesis (Corbett et al., 2013).

4. Discussion

4.1 Source

The Changuinola peat deposit is important as an internationally protected wetland and is an example of a pristine undisturbed functioning tropical peatland. This is supported by the age-depth profiles that showed continuous undisturbed peat accumulation over time, and similarities in C and N concentrations and C:N ratios to other ombrotrophic peat domes across the tropics (Beilman et al., 2019; Omar et al., 2022; Dargie et al., 2017; Lähteenoja et al., 2012). This paper contributes a novel characterization of the organic components contributing to surface CO_2 fluxes (bulk peat, respiration products, peat chemical composition) to identify the dominant source of C for a tropical peatland. Across all sites and depths, DOC was enriched in radiocarbon relative to the bulk peat indicating that it is largely derived from recent photosynthate as opposed to the solid peat, which became progressively older solid peat at depth. Similar behaviour has been reported in other tropical peatlands that preferentially use modern DOC as the source for microbial respiration (Hoyt et al., 2020), while one site in Borneo reported respiration products from mixed sources (Hoyt, 2014). These contrasting results suggest either the Borneo peatland site is an

https://doi.org/10.5194/egusphere-2024-1279
Preprint. Discussion started: 13 May 2024

exception to this behaviour or there is need to explore more tropical peatland sites to characterize source selection behaviour in the tropics. While the microbial utilization of surface DOC deep in the soil profile was seen at our sites, which have contrasting surface vegetation (*Raphia taedigera* vs. mixed hard wood), it is important to note that the preference of surface derived DOC may be related to these being two wood dominated locations. Tropical peatlands with higher abundance of sedge or shrub species may display different source selection preference compared to woody peats based on DOC, root exudate, and peat composition differences (Waldron et al., 2019; Girkin et al., 2018a).

4.2 Peat Chemistry and Stabilization

The dominant biomolecule making up this peat C was lignin, which generally represented >60% of the C in our samples. Despite the lack of a depth difference in the aromaticity index, we saw an accumulation of lignin with depth, indicating preferential preservation of this biomolecule and microbial discrimination against its decomposition through time. This selective preservation of lignin has been reported for this wetland (Hoyos-Santillan et al., 2016) and other tropical peatlands (Gandois et al., 2014) previously, and supports a paradigm of selective preservation of aromatic compounds under anaerobic conditions. Coarse woody material from fallen trees, branches, and dead roots contribute a large yet relatively sporadic portion of C inputs to tropical peat, in addition to the more constant inputs from leaf litter and fine root turnover (Hodgkins et al., 2018), and our data together with the previous studies indicate that this large-scale treen mortality and branch shedding is crucial for peat C accumulation. The waterlogged conditions in tropical peatlands can particularly reduce the decomposition of lignin by inhibiting ligninolytic microbes (Thormann, 2006; Hoyos-Santillan et al., 2015). There was little change in the carbohydrate portion of peat C with depth, even though carbohydrates typically represent the most labile compounds in plant tissues for decomposition (Bader et al., 2018). This lack of change in carbohydrate abundance with depth below 30 cm may indicate consistent preservation of this molecule after any initial decomposition in the top 30 cm, and contrasts with the preferential preservation of lignin. Interestingly, we see a significant decline in lipids with depth, even though other tropical and temperate forest studies have indicated preferential preservation of lipids in upland soils (Cusack et al., 2018; Wiesenberg et al., 2010; Jastrow et al., 2007). Our data suggest that under anaerobic conditions, lipids are decomposed more than other compounds, and/or microbial biomass production of lipids declines, or changes in carbon inputs over time. Taken together, our data support different decomposition rates and preservation processes of individual biomarkers that contribute to the accumulation of organic C within tropical peatlands (Girkin et al., 2018a; Hoyos-Santillan et al., 2015, 2016).

Our outer site is closest to the edge of the peatland in an area in the peatland that is dominated by *Raphia taedigera* palm swamp and with relatively high nutrient availability, while the intermediate site dominated by mixed forest swamp species, and the inner site closest to the centre of the peatland dominated by stunted *Campnosperma panamensis* forest and has relatively low nutrient availability (Troxler, 2007; Phillips and Bustin, 1996; Sjögersten et al., 2011). Despite these documented differences, we found strong similarity across sites in peat characteristics as well as the radiocarbon content of porewater DOC, CO_2, and CH_4. Our results demonstrate that the peat at or below 2 m is relatively carbohydrate- and lignin-rich and potentially less decomposed than expected, making these soils vulnerable to rapid decomposition if exposed to aerobic conditions.

https://doi.org/10.5194/egusphere-2024-1279
Preprint. Discussion started: 13 May 2024

Based on the ^{14}C and age of peat collected across these sites, the dome shape of the peatland has built up with older layers closer to the surface at the margins (Fig 8). This shape and accumulation pattern has been described and modelled across other tropical peat domes that have the similar ombrotrophic characteristics as Changuinola (Cobb et al., 2017). Our results suggest age was not a driver of peat chemical characteristics or properties that describe decomposability, and that older peat that accumulated over 1000 years ago is closer to the surface at the margins and would be the first layers to experience aerobic conditions with changes in water table draw down or disturbance (Dommain et al., 2011).

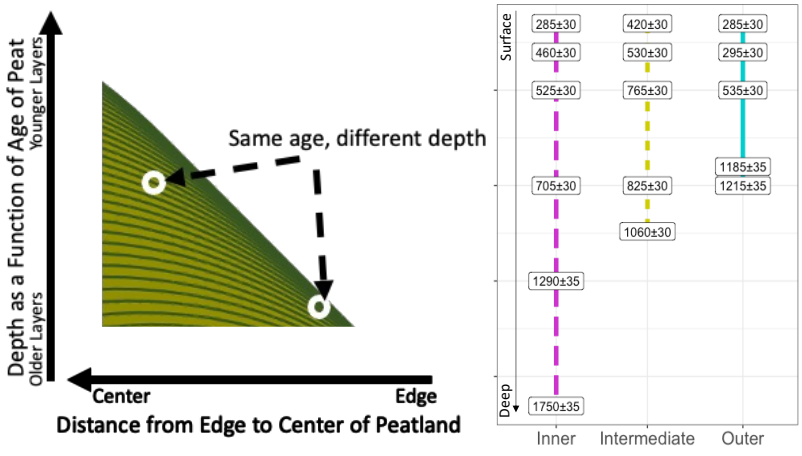

Figure 8: Schematic of peatland shape and layer accumulation pattern based on peat layer age and depth from surface. This concept was presented in model data from Cobb et al., 2017 and has been modified to create this schematic that is not to scale. Peat layers accumulate over time with the youngest layers at the surface and oldest layers at the base of the peat deposit. Based on this and ages collected from the sites within the Changuinola peat deposit, layers that correspond to the same age are located at different depths across the peat dome with older peat layers are closer to the surface at the margins.

Using $\delta^{13}C$ to understand CH_4 Production

Peat organic matter quality influences not only decomposition rates but also the CH_4 production pathway (Holmes et al., 2015). When easily degradable inputs are decomposed, acetate is produced by fermentative bacteria, increasing the importance of acetoclastic methanogenesis (Mobilian and Craft, 2022). After the labile material is depleted, the decomposition of more resistant material and related CO_2 production leads to an increase in importance of hydrogenotrophic methanogenesis (Conrad, 2020). The high αapp (1.078 ± 0.003) observed here indicates that hydrogenotrophic methanogenesis is the dominant production pathway with no signs of depth distribution. While this study is unable to map the exact progression of the fermentation process from original plant material to CH_4, we know hydrogenotrophic methanogenesis is only possible with the availability of CO_2 for reduction to CH, and that CO_2 produced in the initial steps of decomposition is a strong potential supply of CO_2 to support hydrogenotrophic methanogenesis (Kotsyurbenko et al., 2004; Gruca-Rokosz and Koszelnik, 2018). This cooperation between microbial communities, where initial degraders provide necessary precursors (in this case CO_2 from decomposition) for further microbial metabolism by other communities, has been observed in soils and could be a mechanism

https://doi.org/10.5194/egusphere-2024-1279
Preprint. Discussion started: 13 May 2024

regulating the release of CO_2 in this peatland (Chen et al., 2023; Li et al., 2021). Further work is needed to explore the methanogen community composition and stratigraphy that might affect net CH_4 flux from this wetland and determine potential surface processes that would cause a shift in CH_4 production pathway in surface (0-30cm) peat.

Future Implications

Tropical peatlands are important C rich ecosystems that are vulnerable to future change. Here, we described how sites within a peatland with varied surface vegetation and nutrient status all preferentially support deep peat respiration with surface derived DOC, produce CH_4 via hydrogenotrophic methanogenesis, and continue to accumulate C dense bulk peat. We found that the bulk peat currently saturated in the Changuinola peatland is primarily comprised of lignin, with accumulation of lignin at depth, presumably because of microbial discrimination against its decomposition in anaerobic conditions. It is unclear how resistant to decomposition this lignin would be if exposed to aerobic conditions. Changes in climate and drying of peatlands will expose C that has been preserved under anaerobic conditions to rapid microbial decomposition. Vegetation shifts and drops in water table depth that can also disconnect the surface from deep peat layers and expose peat previously preserved by anoxic conditions to rapid, aerobic decomposition (Kettridge et al., 2015; Ofiti et al., 2023). Shifts in composition, availability or amounts of inputs from the surface will influence greenhouse gas production in ways that are not straightforward or direct, and there is a need and plenty of room to further study these relationships. Taken together, these results make it clear that this peatland is storing and protecting peat C under current conditions. However, based on the importance of DOC transport and deep peat preservation and decay dynamics, changes in precipitation and evapotranspiration that influence transport and connectivity between surface and deep peat could greatly impact the C storage capacity of this ecosystem.

https://doi.org/10.5194/egusphere-2024-1279
Preprint. Discussion started: 13 May 2024

370 **Appendix A**

Table A1: **Radiocarbon results for both untreated (No Acid-Base-Acid) and treated (Acid-Base-Acid) sets of peat samples**. Radiocarbon concentration is expressed as $\Delta^{14}C$ within two standard deviations.

Site	Depth	$\Delta^{14}C$ (No ABA)	±	$\Delta^{14}C$ (ABA)	±
Outer	100	-72.4	3.1	-77.5	4.0
	180	-147.8	3.2	-157.6	3.6
	200	-144.3	3.2	-157.8	3.6
	30	-43.1	3.4	-54.9	4.1
	60	-44.0	3.4	-54.2	4.1
Intermediate	30	-59.2	3.4	-59.9	4.0
	60	-71.8	3.3	-70.2	4.0
	100	-98.8	3.3	-107.5	3.8
	200	-105.1	3.2	-110.8	3.8
	248	-130.8	3.2	-141.0	3.7
Inner	30	-42.9	3.3	-45.6	4.1
	60	-63.3	3.3	-68.5	4.0
	100	-71.0	3.2	-75.9	4.0
	200	-92.0	3.3	-93.6	3.9
	300	-155.8	3.2	-155.2	3.6
	431	-202.7	3.1	-203.1	3.4

375

380

https://doi.org/10.5194/egusphere-2024-1279
Preprint. Discussion started: 13 May 2024

Table A2: **Mixing model outputs for all depths sampled from the three sites.** Molecular component proportion of total C measured via ^{13}CNMR described by the mixing model output as weighted percent (Wt%) developed by Baldock et al., 2004, %C measured from bulk peat combustion via elemental analyzer.

Site	**Depth**	**Molecular Component**	Wt%	**%C**
Inner	30	Carbohydrate	16.5	54.33
Inner	30	Protein	12.9	54.33
Inner	30	Lignin	61.0	54.33
Inner	30	Lipid	9.6	54.33
Inner	30	Carbonyl	0.0	54.33
Inner	60	Carbohydrate	13.9	55.49
Inner	60	Protein	9.6	55.49
Inner	60	Lignin	66.3	55.49
Inner	60	Lipid	6.4	55.49
Inner	60	Carbonyl	3.8	55.49
Inner	100	Carbohydrate	13.4	53.24
Inner	100	Protein	12.1	53.24
Inner	100	Lignin	65.3	53.24
Inner	100	Lipid	8.5	53.24
Inner	100	Carbonyl	0.7	53.24
Inner	200	Carbohydrate	13.0	54.87
Inner	200	Protein	12.1	54.87
Inner	200	Lignin	64.0	54.87
Inner	200	Lipid	5.7	54.87
Inner	200	Carbonyl	5.3	54.87
Inner	300	Carbohydrate	14.9	54.88
Inner	300	Protein	14.8	54.88
Inner	300	Lignin	62.6	54.88
Inner	300	Lipid	7.7	54.88

https://doi.org/10.5194/egusphere-2024-1279
Preprint. Discussion started: 13 May 2024

Inner	300	Carbonyl	0.0	54.88
Inner	431	Carbohydrate	16.3	47.91
Inner	431	Protein	9.9	47.91
Inner	431	Lignin	71.6	47.91
Inner	431	Lipid	2.2	47.91
Inner	431	Carbonyl	0.0	47.91
Intermediate	30	Carbohydrate	17.4	55.01
Intermediate	30	Protein	13.5	55.01
Intermediate	30	Lignin	54.5	55.01
Intermediate	30	Lipid	14.5	55.01
Intermediate	30	Carbonyl	0.0	55.01
Intermediate	60	Carbohydrate	19.6	54.84
Intermediate	60	Protein	13.8	54.84
Intermediate	60	Lignin	58.2	54.84
Intermediate	60	Lipid	8.4	54.84
Intermediate	60	Carbonyl	0.0	54.84
Intermediate	100	Carbohydrate	15.8	53.76
Intermediate	100	Protein	11.7	53.76
Intermediate	100	Lignin	64.8	53.76
Intermediate	100	Lipid	7.7	53.76
Intermediate	100	Carbonyl	0.0	53.76
Intermediate	200	Carbohydrate	15.9	52.96
Intermediate	200	Protein	12.3	52.96
Intermediate	200	Lignin	64.9	52.96
Intermediate	200	Lipid	7.0	52.96
Intermediate	200	Carbonyl	0.0	52.96
Intermediate	248	Carbohydrate	17.3	39.96

https://doi.org/10.5194/egusphere-2024-1279
Preprint. Discussion started: 13 May 2024

Intermediate	248	Protein	9.3	39.96
Intermediate	248	Lignin	72.4	39.96
Intermediate	248	Lipid	1.0	39.96
Intermediate	248	Carbonyl	0.0	39.96
Outer	30	Carbohydrate	19.9	53.92
Outer	30	Protein	14.4	53.92
Outer	30	Lignin	59.5	53.92
Outer	30	Lipid	6.2	53.92
Outer	30	Carbonyl	0.0	53.92
Outer	60	Carbohydrate	18.1	52.40
Outer	60	Protein	16.8	52.40
Outer	60	Lignin	60.2	52.40
Outer	60	Lipid	5.0	52.40
Outer	60	Carbonyl	0.0	52.40
Outer	100	Carbohydrate	18.1	53.60
Outer	100	Protein	16.8	53.60
Outer	100	Lignin	60.2	53.60
Outer	100	Lipid	5.0	53.60
Outer	100	Carbonyl	0.0	53.60
Outer	180	Carbohydrate	22.4	39.96
Outer	180	Protein	9.4	39.96
Outer	180	Lignin	68.2	39.96
Outer	180	Lipid	0.0	39.96
Outer	180	Carbonyl	0.0	39.96
Outer	200	Carbohydrate	21.0	45.03
Outer	200	Protein	7.5	45.03
Outer	200	Lignin	69.4	45.03

https://doi.org/10.5194/egusphere-2024-1279
Preprint. Discussion started: 13 May 2024

Outer	200	Lipid	0.0	45.03
Outer	200	Carbonyl	2.2	45.03

https://doi.org/10.5194/egusphere-2024-1279
Preprint. Discussion started: 13 May 2024

Fig A1

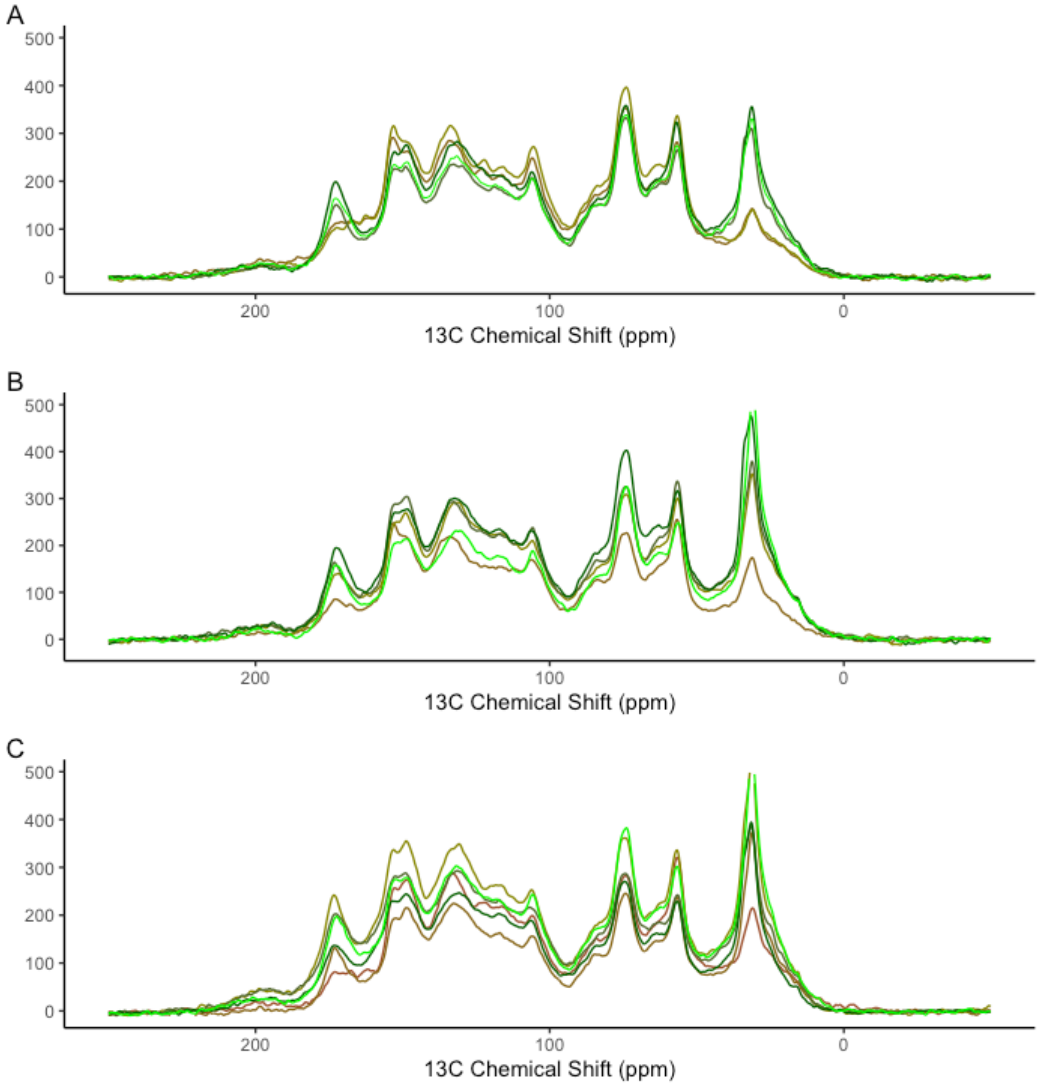

Fig A2: Stacked overlay of depth profiles of ^{13}C NMR spectra of the A) Outer, B) Intermediate, and C) Inner site. Colors increase in darkness representing an increase in depth with light green being the 30cm material and dark brown being the basal material. Spectra were digitally processed with Mnova software (v. 14.3.3; Mestrelab Research) with exponential apodization (100 Hz line broadening with the first point set to 0.50), phase correction, and baseline correction using a Bernstein polynomial fit. Peak areas were integrated corresponding to; alkyl C (0–45 ppm), N-alkyl/methoxyl C (45–60 ppm), O-alkyl C (60–95 ppm), di-O-alkyl (95–110), aromatic C (110–145 ppm), phenolic C (145-165 ppm), and carboxyl C (165–215 ppm).

390

https://doi.org/10.5194/egusphere-2024-1279
Preprint. Discussion started: 13 May 2024

Fig A2

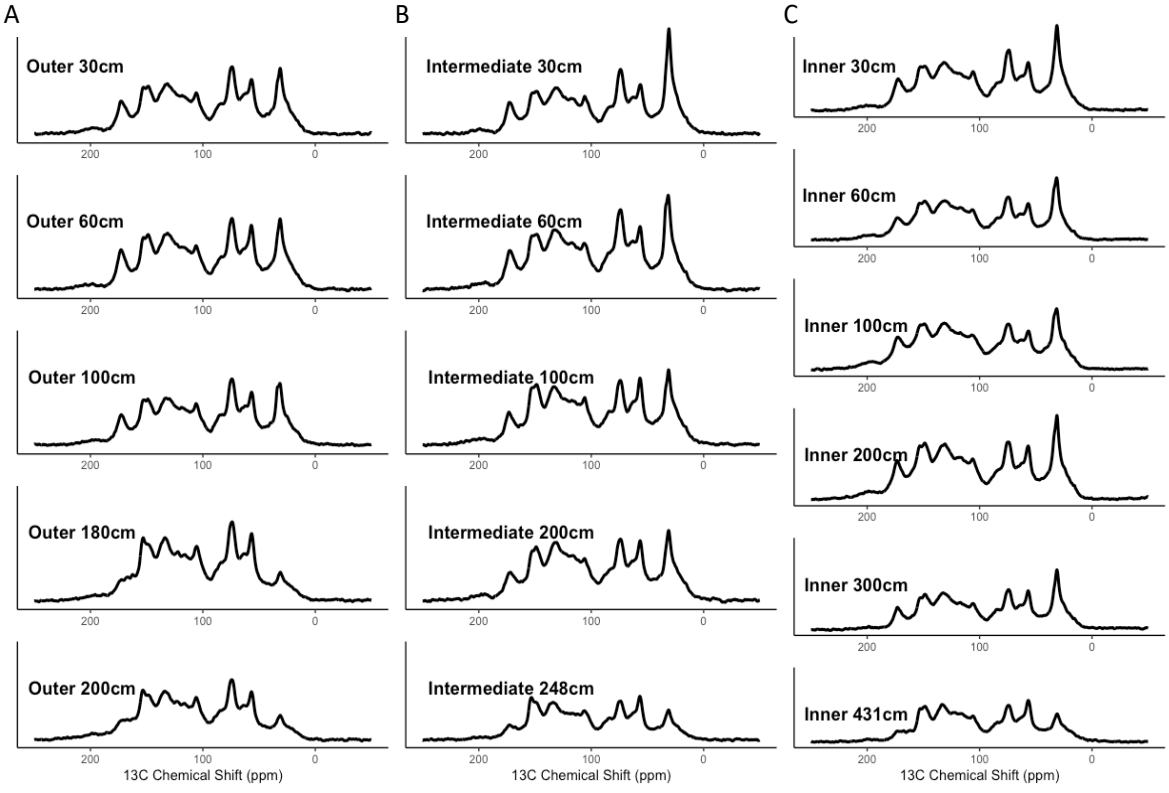

Fig A3: Depth profiles of 13C NMR spectra for the A) Outer, B) Intermediate, and C) Inner sites. Spectra were digitally processed with Mnova software (v. 14.3.3; Mestrelab Research) with exponential apodization (100 Hz line broadening with the first point set to 0.50), phase correction, and baseline correction using a Bernstein polynomial fit. Peak areas were integrated corresponding to; alkyl C (0–45 ppm), N-alkyl/methoxyl C (45–60 ppm), O-alkyl C (60–95 ppm), di-O-alkyl (95–110), aromatic C (110–145 ppm), phenolic C (145-165 ppm), and carboxyl C (165–215 ppm). The y-axis has been scaled equally across all plots to visually compare changes in peak heights and area across depth, however the additional depths at the Inner site need to be considered when comparing across sites.

https://doi.org/10.5194/egusphere-2024-1279
Preprint. Discussion started: 13 May 2024

395

400

405 **Table A3: Results from two-sample t-tests** comparing bulk peat radiocarbon vaues versus respiration product radiocarbon values, and DOC radiocarbon values versus respiration product radiocarbon values.

	Sample Type	Mean	t-value	df	p-value
Pair 1	Bulk Peat	-96.5625	-8.6657	15.974	1.96E-07
	Gases (CH4, CO2)	7.95			
Pair 2	DOC	2.027273	0.53811	23	0.5957
	Gases (CH4, CO2)	-3.878571			

https://doi.org/10.5194/egusphere-2024-1279
Preprint. Discussion started: 13 May 2024

410

Fig A3

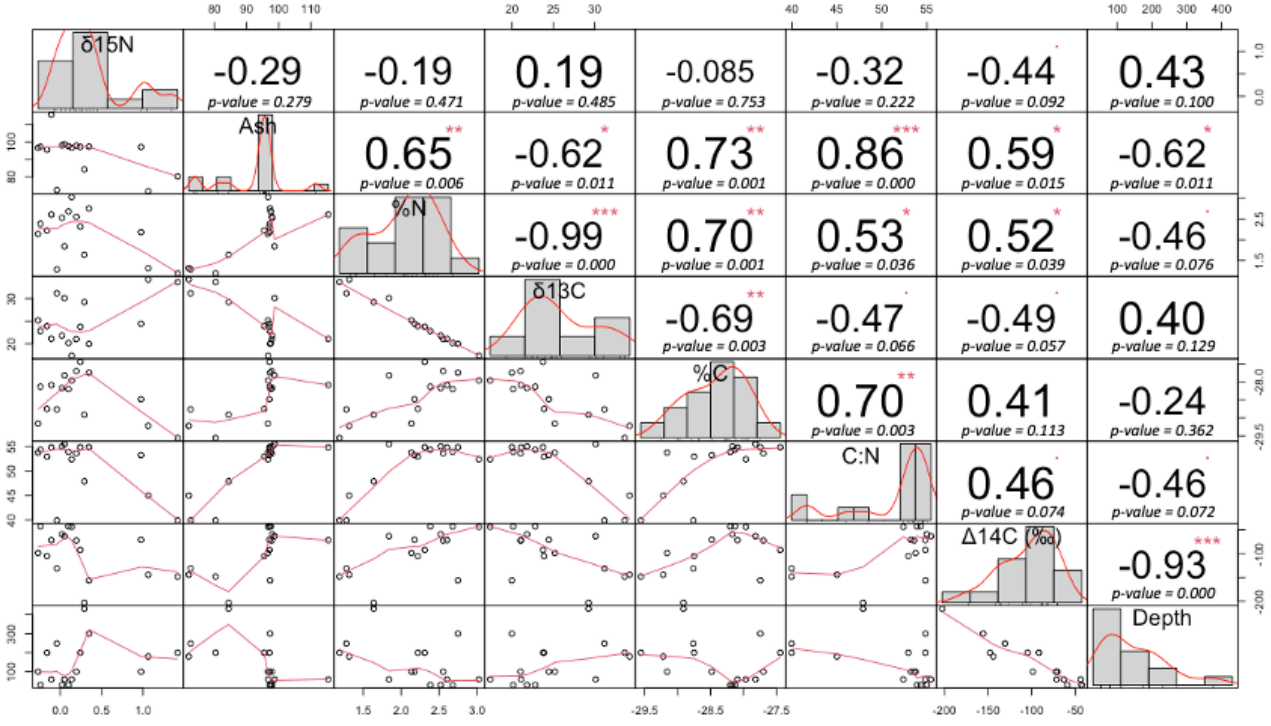

Fig A3: Correlation matrix for peat physical properties and depth. The numbers represent the value of the correlation coefficient (r) plus the result of the cor.test as stars. On the bottom of the matrix are the bivariate scatterplots with a fitted line. Significand codes: 0 '*' 0.001 '**' 0.01 '*' 0.1 ' '.**

https://doi.org/10.5194/egusphere-2024-1279
Preprint. Discussion started: 13 May 2024

Fig A4

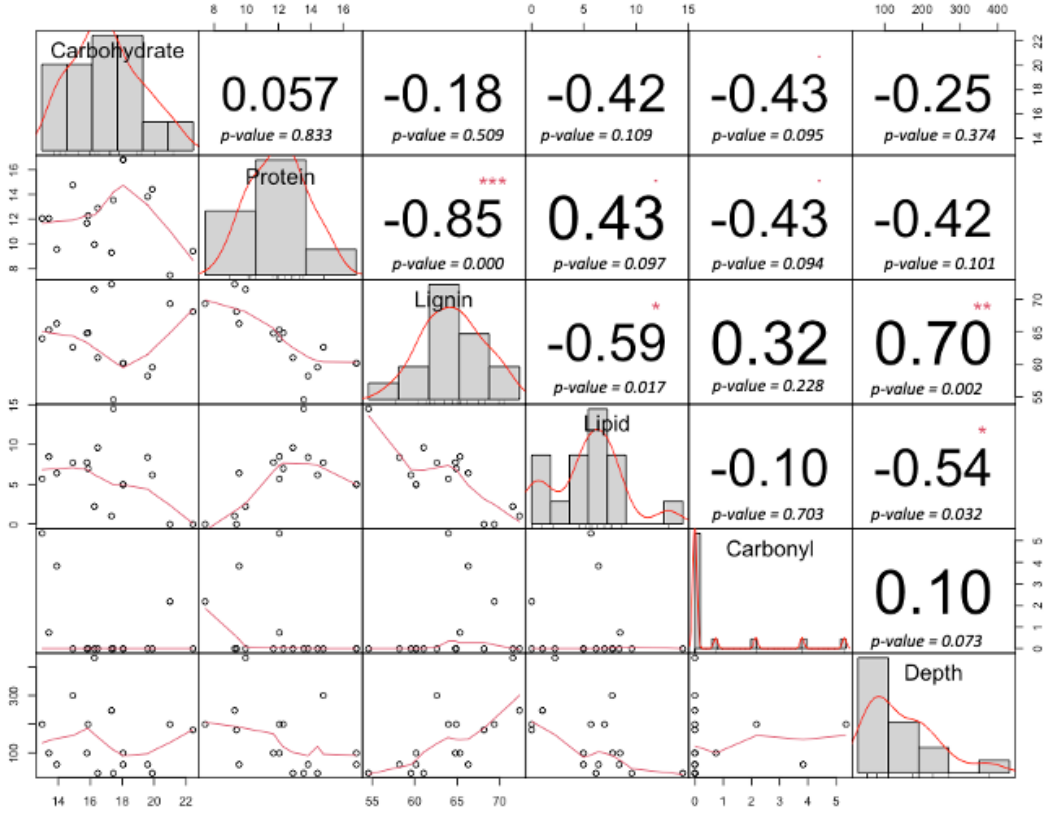

Fig A4: Correlation matrix for peat molecular components and depth. The numbers represent the value of the correlation (r^2) plus the result of the cor.test as stars. On the bottom of the matrix are the bivariate scatterplots with a fitted line. Significand codes: 0 '*' 0.001 '**' 0.01 '*' 0.1 ''.**

https://doi.org/10.5194/egusphere-2024-1279
Preprint. Discussion started: 13 May 2024

415

Table A4: PCA eigenvalues and loadings for PC1 and PC2.

	PC1	**PC2**
Eigenvalues	**3.314e+00**	**1.941e+00**
Variable		
δ15N	-0.186	0.039
Ash	-0.386	-0.077
%N	0.274	-0.109
δ13C	0.230	0.165
%C	0.275	0.091
C:N	-0.266	0.144
Δ14C (‰)	0.233	0.035
Depth	-0.191	0.011
LOI	0.265	-0.008
Alkyl	0.284	-0.041
N-Alkyl/Methoxyl	-0.129	-0.402
O-Alkyl	-0.156	-0.325
Di_O_Alkyl	-0.273	-0.027
Aromatic	-0.251	0.034
Phenolic	-0.230	0.296
Amide/Carboxyl	0.094	0.414
Carbohydrate	-0.121	-0.344
Protein	0.236	-0.200
Lignin	-0.264	0.157
Lipid	0.263	-0.015
Carbonyl	-0.005	0.464

https://doi.org/10.5194/egusphere-2024-1279
Preprint. Discussion started: 13 May 2024

Fig A5

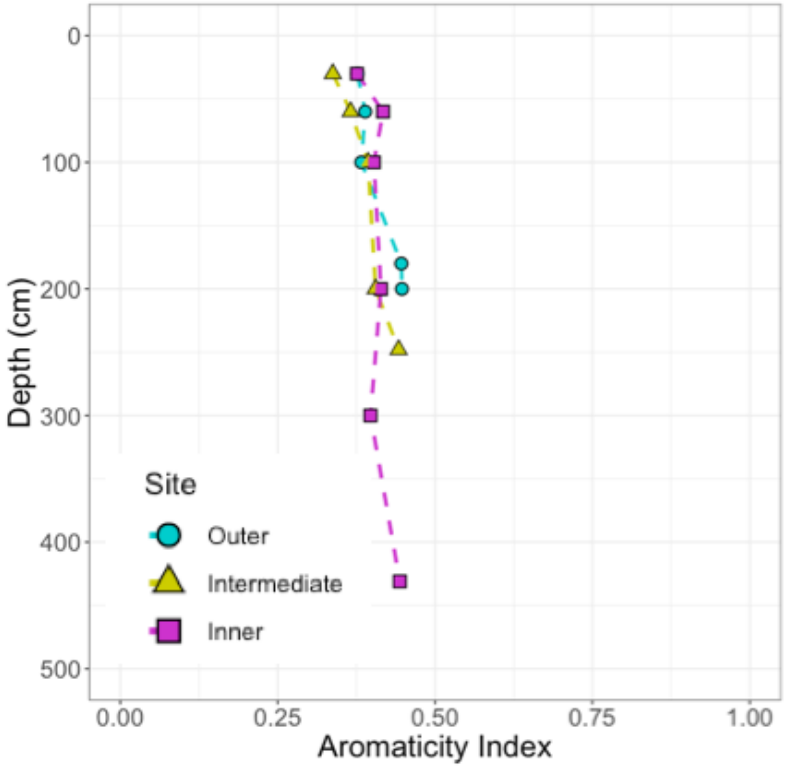

Fig A5: Aromaticity Index. The aromaticity index has been used to describe decomposition state of soils. This index is expressed as the ratio of Aromatic-C to Alkyl + O-Alkyl + Aromatic C and is calculated using the results from integration of the ^{13}C NMR spectra. As the aromaticity index approaches 1, the soil is considered more decomposed. The lack of change in aromaticity with depth, and the consistency across all three sites, suggests little decomposition has occurred over space and time. Sites are indicated by color and shape with blue circles indicating the outer site, yellow triangles the intermediate site, and pink squares the inner site.

https://doi.org/10.5194/egusphere-2024-1279
Preprint. Discussion started: 13 May 2024

Fig A6

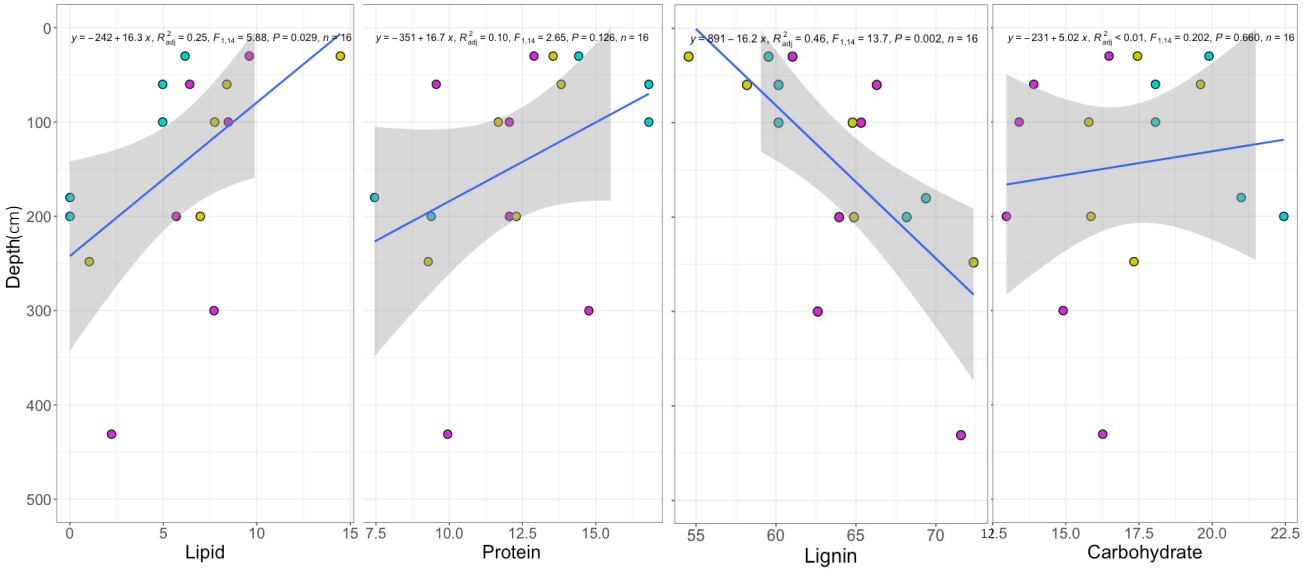

Fig A6: Linear regression of the four most abundant biomolecules from the mixing model versus depth. Sites have been pooled for this analysis but are indicated by color with blue indicating the outer site, yellow the intermediate site, and pink the inner site. Regressions show significant declines with depth for lipids, and significant increases with depth for lignin across sites.

https://doi.org/10.5194/egusphere-2024-1279
Preprint. Discussion started: 13 May 2024

Author Contribution

Alexandra Hedgpeth: Conceptualization; funding acquisition; data collection; formal analysis; investigation; methodology; visualization; writing – original draft. **Alison Hoyt:** Methodology; resources; formal analysis; visualization; supervision; writing – review and editing. **Daniela Cusack:** Conceptualization; funding acquisition; methodology; supervision; visualization; writing – review and editing. **Kyle Cavanaugh:** Supervision; writing – review and editing. **Karis McFarlane:** Funding acquisition; resources; methodology; supervision; writing – review and editing. Karis J. McFarlane and Daniela F. Cusack should be considered joint senior authors.

Data Availability

Following publication, the data that supports this manuscript will be publicly available at the US Department of Energy's Environmental Systems Science Data Infrastructure for a Virtual Ecosystem (ESS-DIVE: https://ess-dive.lbl.gov/) and will be submitted to the International Soil Radiocarbon Database (https://soilradiocarbon.org/).

Competing interests

The contact author has declared that none of the authors has any competing interests.

Acknowledgements

A. Hedgpeth thanks the Smithsonian Tropical Research Institute for a short-term research fellowship, Eric Brown for field support, and the staff at the Smithsonian Tropical Research Institute and the Bocas del Toro field station for logistical support. This project was supported in part by a University of California-National Lab In-Residence Graduate Fellowship (#L21GF3629) to A. Hedgpeth, which was hosted by Lawrence Livermore National Laboratory. The ^{13}C-NMR analysis for this work was supported under a U.S. Department of Energy User Award (#60514) to D. Cusack and A. Hedgpeth, which was conducted at the Environmental Molecular Sciences Laboratory. Access to field and lab sites in Panama was supported by DOE Office of Science Early Career Award DE-SC0015898 and NSF Geography & Spatial Studies Grant #BCS-1437591 to D. Cusack. We would like to thank Sarah Burton and Andrew Lipton from the Environmental Molecular Sciences Laboratory for their assistance with the ^{13}C-NMR analysis. A portion of this work was performed under the auspices of the U.S. Department of Energy by Lawrence Livermore National Laboratory under Contract DE-AC52-07NA27344 and funded by the U.S. Department of Energy Office of Science Early Career Program Award (#SCW1572) to K. McFarlane. We would like to thank Antonia L. Herwig, Lee Dietterich, and Makenna Brown for their assistance in the field.

References

Aliev, A. E.: Solid state NMR spectroscopy, in: Nuclear Magnetic Resonance, edited by: Hodgkinson, P., The Royal Society of Chemistry, 139–187, https://doi.org/10.1039/9781788010665-00139, 2020.

https://doi.org/10.5194/egusphere-2024-1279
Preprint. Discussion started: 13 May 2024

Anderson, J. A. R. and Muller, J.: Palynological study of a holocene peat and a miocene coal deposit from NW Borneo, Review of Palaeobotany and Palynology, 19, 291–351, https://doi.org/10.1016/0034-6667(75)90049-4, 1975.

Aravena, R., Warner, B. G., Charman, D. J., Belyea, L. R., Mathur, S. P., and Dinel, H.: Carbon Isotopic Composition of Deep Carbon Gases in an Ombrogenous Peatland, Northwestern Ontario, Canada, Radiocarbon, 35, 271–276, https://doi.org/10.1017/S0033822200064948, 1993.

Bader, C., Müller, M., Schulin, R., and Leifeld, J.: Peat decomposability in managed organic soils in relation to land use, organic matter composition and temperature, Biogeosciences, 15, 703–719, https://doi.org/10.5194/bg-15-703-2018, 2018.

Baldock, J. A., Masiello, C. A., Gélinas, Y., and Hedges, J. I.: Cycling and composition of organic matter in terrestrial and marine ecosystems, Marine Chemistry, 92, 39–64, https://doi.org/10.1016/j.marchem.2004.06.016, 2004.

Barreto, C. and Lindo, Z.: Decomposition in Peatlands: Who Are the Players and What Affects Them?, Front. Young Minds, 8, 107, https://doi.org/10.3389/frym.2020.00107, 2020.

Beilman, D. W., Massa, C., Nichols, J. E., Elison Timm, O., Kallstrom, R., and Dunbar-Co, S.: Dynamic Holocene Vegetation and North Pacific Hydroclimate Recorded in a Mountain Peatland, Moloka‘i, Hawai‘i, Front. Earth Sci., 7, 188, https://doi.org/10.3389/feart.2019.00188, 2019.

Broek, T. A. B., Ognibene, T. J., McFarlane, K. J., Moreland, K. C., Brown, T. A., and Bench, G.: Conversion of the LLNL/CAMS 1 MV biomedical AMS system to a semi-automated natural abundance 14C spectrometer: system optimization and performance evaluation, Nuclear Instruments and Methods in Physics Research Section B: Beam Interactions with Materials and Atoms, 499, 124–132, https://doi.org/10.1016/j.nimb.2021.01.022, 2021.

Chanton, J. P., Glaser, P. H., Chasar, L. S., Burdige, D. J., Hines, M. E., Siegel, D. I., Tremblay, L. B., and Cooper, W. T.: Radiocarbon evidence for the importance of surface vegetation on fermentation and methanogenesis in contrasting types of boreal peatlands, Global Biogeochemical Cycles, 22, 2008GB003274, https://doi.org/10.1029/2008GB003274, 2008.

Charman, D. J., Aravena, R., Bryant, C. L., and Harkness, D. D.: Carbon isotopes in peat, DOC, CO2, and CH4 in a Holocene peatland on Dartmoor, southwest England, Geol, 27, 539, https://doi.org/10.1130/0091-7613(1999)027<0539:CIIPDC>2.3.CO;2, 1999.

Chen, X., Xue, D., Wang, Y., Qiu, Q., Wu, L., Wang, M., Liu, J., and Chen, H.: Variations in the archaeal community and associated methanogenesis in peat profiles of three typical peatland types in China, Environmental Microbiome, 18, 48, https://doi.org/10.1186/s40793-023-00503-y, 2023.

Clymo, R. S., Turunen, J., and Tolonen, K.: Carbon Accumulation in Peatland, Oikos, 81, 368, https://doi.org/10.2307/3547057, 1998.

Cobb, A. R., Hoyt, A. M., Gandois, L., Eri, J., Dommain, R., Abu Salim, K., Kai, F. M., Haji Su'ut, N. S., and Harvey, C. F.: How temporal patterns in rainfall determine the geomorphology and carbon fluxes of tropical peatlands, Proc. Natl. Acad. Sci. U.S.A., 114, https://doi.org/10.1073/pnas.1701090114, 2017.

Cohen, A. D., Raymond, R., Ramirez, A., Morales, Z., and Ponce, F.: The Changuinola peat deposit of northwestern Panama: a tropical, back-barrier, peat(coal)-forming environment, International Journal of Coal Geology, 12, 157–192, https://doi.org/10.1016/0166-5162(89)90050-5, 1989.

Corbett, J. E.: DOC reactivity in a northern Minnesota peatland, Phd dissertation, 2012.

https://doi.org/10.5194/egusphere-2024-1279
Preprint. Discussion started: 13 May 2024

Corbett, J. E., Tfaily, M. M., Burdige, D. J., Cooper, W. T., Glaser, P. H., and Chanton, J. P.: Partitioning pathways of CO2 production in peatlands with stable carbon isotopes, Biogeochemistry, 114, 327–340, https://doi.org/10.1007/s10533-012-9813-1, 2013.

Dargie, G. C., Lewis, S. L., Lawson, I. T., Mitchard, E. T. A., Page, S. E., Bocko, Y. E., and Ifo, S. A.: Age, extent and carbon storage of the central Congo Basin peatland complex, Nature, 542, 86–90, https://doi.org/10.1038/nature21048, 2017.

Dhandapani, S., Girkin, N. T., and Evers, S.: Spatial variability of surface peat properties and carbon emissions in a tropical peatland oil palm monoculture during a dry season, Soil Use and Management, 38, 381–395, https://doi.org/10.1111/sum.12741, 2022.

Dhandapani, S., Evers, S., Boyd, D., Evans, C. D., Page, S., Parish, F., and Sjogersten, S.: Assessment of differences in peat physico-chemical properties, surface subsidence and GHG emissions between the major land-uses of Selangor peatlands, CATENA, 230, 107255, https://doi.org/10.1016/j.catena.2023.107255, 2023.

Dommain, R., Cobb, A. R., Joosten, H., Glaser, P. H., Chua, A. F. L., Gandois, L., Kai, F., Noren, A., Salim, K. A., Su'ut, N. S. H., and Harvey, C. F.: Forest dynamics and tip-up pools drive pulses of high carbon accumulation rates in a tropical peat dome in Borneo (Southeast Asia), JGR Biogeosciences, 120, 617–640, https://doi.org/10.1002/2014JG002796, 2015.

Drollinger, S., Kuzyakov, Y., and Glatzel, S.: Effects of peat decomposition on δ13C and δ15N depth profiles of Alpine bogs, CATENA, 178, 1–10, https://doi.org/10.1016/j.catena.2019.02.027, 2019.

Farmer, J., Matthews, R., Smith, J. U., Smith, P., and Singh, B. K.: Assessing existing peatland models for their applicability for modelling greenhouse gas emissions from tropical peat soils, Current Opinion in Environmental Sustainability, 3, 339–349, https://doi.org/10.1016/j.cosust.2011.08.010, 2011.

Fritts, R.: Tropical Wetlands Emit More Methane Than Previously□Thought, Eos, 103, https://doi.org/10.1029/2022EO220443, 2022.

Gandois, L., Teisserenc, R., Cobb, A. R., Chieng, H. I., Lim, L. B. L., Kamariah, A. S., Hoyt, A., and Harvey, C. F.: Origin, composition, and transformation of dissolved organic matter in tropical peatlands, Geochimica et Cosmochimica Acta, 137, 35–47, https://doi.org/10.1016/j.gca.2014.03.012, 2014.

Girkin, N. T., Turner, B. L., Ostle, N., Craigon, J., and Sjögersten, S.: Root exudate analogues accelerate CO2 and CH4 production in tropical peat, Soil Biology and Biochemistry, 117, 48–55, https://doi.org/10.1016/j.soilbio.2017.11.008, 2018.

Girkin, N. T., Vane, C. H., Cooper, H. V., Moss-Hayes, V., Craigon, J., Turner, B. L., Ostle, N., and Sjögersten, S.: Spatial variability of organic matter properties determines methane fluxes in a tropical forested peatland, Biogeochemistry, 142, 231–245, https://doi.org/10.1007/s10533-018-0531-1, 2019.

Girkin, N. T., Dhandapani, S., Evers, S., Ostle, N., Turner, B. L., and Sjögersten, S.: Interactions between labile carbon, temperature and land use regulate carbon dioxide and methane production in tropical peat, Biogeochemistry, 147, 87–97, https://doi.org/10.1007/s10533-019-00632-y, 2020.

Girkin, N. T., Cooper, H. V., Ledger, M. J., O'Reilly, P., Thornton, S. A., Åkesson, C. M., Cole, L. E. S., Hapsari, K. A., Hawthorne, D., and Roucoux, K. H.: Tropical peatlands in the Anthropocene: The present and the future, Anthropocene, 40, 100354, https://doi.org/10.1016/j.ancene.2022.100354, 2022.

Goldstein, A., Turner, W. R., Spawn, S. A., Anderson-Teixeira, K. J., Cook-Patton, S., Fargione, J., Gibbs, H. K., Griscom, B., Hewson, J. H., Howard, J. F., Ledezma, J. C., Page, S., Koh, L. P., Rockström, J., Sanderman, J., and Hole, D. G.: Protecting

https://doi.org/10.5194/egusphere-2024-1279
Preprint. Discussion started: 13 May 2024

irrecoverable carbon in Earth's ecosystems, Nat. Clim. Chang., 10, 287–295, https://doi.org/10.1038/s41558-020-0738-8, 2020.

Gruca-Rokosz, R. and Koszelnik, P.: Production pathways for CH4 and CO2 in sediments of two freshwater ecosystems in south-eastern Poland, PLoS ONE, 13, e0199755, https://doi.org/10.1371/journal.pone.0199755, 2018.

Hirano, T., Jauhiainen, J., Inoue, T., and Takahashi, H.: Controls on the Carbon Balance of Tropical Peatlands, Ecosystems, 12, 873–887, https://doi.org/10.1007/s10021-008-9209-1, 2009.

Hobbie, E. A. and Ouimette, A. P.: Controls of nitrogen isotope patterns in soil profiles, Biogeochemistry, 95, 355–371, https://doi.org/10.1007/s10533-009-9328-6, 2009.

Hodgkins, S. B., Richardson, C. J., Dommain, R., Wang, H., Glaser, P. H., Verbeke, B., Winkler, B. R., Cobb, A. R., Rich, V. I., Missilmani, M., Flanagan, N., Ho, M., Hoyt, A. M., Harvey, C. F., Vining, S. R., Hough, M. A., Moore, T. R., Richard, P. J. H., De La Cruz, F. B., Toufaily, J., Hamdan, R., Cooper, W. T., and Chanton, J. P.: Tropical peatland carbon storage linked to global latitudinal trends in peat recalcitrance, Nat Commun, 9, 3640, https://doi.org/10.1038/s41467-018-06050-2, 2018.

Hornibrook, E. R. C., Longstaffe, F. J., and Fyfe, W. S.: Evolution of stable carbon isotope compositions for methane and carbon dioxide in freshwater wetlands and other anaerobic environments, Geochimica et Cosmochimica Acta, 64, 1013–1027, https://doi.org/10.1016/S0016-7037(99)00321-X, 2000a.

Hornibrook, E. R. C., Longstaffe, F. J., and Fyfe, W. S.: Factors Influencing Stable Isotope Ratios in CH_4 and CO_2 Within Subenvironments of Freshwater Wetlands: Implications for δ-Signatures of Emissions, Isotopes in Environmental and Health Studies, 36, 151–176, https://doi.org/10.1080/10256010008032940, 2000b.

Hoyos-Santillan, J.: 2014 Hoyos Controls of Carbon Turnover in Tropical Peatlands, https://doi.org/10.13140/2.1.3387.2329, 2014.

Hoyos-Santillan, J., Lomax, B. H., Large, D., Turner, B. L., Boom, A., Lopez, O. R., and Sjögersten, S.: Quality not quantity: Organic matter composition controls of CO2 and CH4 fluxes in neotropical peat profiles, Soil Biology and Biochemistry, 103, 86–96, https://doi.org/10.1016/j.soilbio.2016.08.017, 2016.

Hoyos-Santillan, J., Lomax, B. H., Large, D., Turner, B. L., Lopez, O. R., Boom, A., Sepulveda-Jauregui, A., and Sjögersten, S.: Evaluation of vegetation communities, water table, and peat composition as drivers of greenhouse gas emissions in lowland tropical peatlands, Science of The Total Environment, 688, 1193–1204, https://doi.org/10.1016/j.scitotenv.2019.06.366, 2019.

Hoyt, A.: Methane production and transport in a tropical peatland, AGU Fall Meeting Abstracts, 2014.

Hoyt, A., Cadillo-Quiroz, H., Xu, X., Torn, M., Bazán Pacaya, A., Jacobs, M., Shapiama Peña, R., Ramirez Navarro, D., Urquiza-Muñoz, D., and Trumbore, S.: Isotopic Insights into Methane Production and Emission in Diverse Amazonian Peatlands, oral, https://doi.org/10.5194/egusphere-egu2020-12960, 2020.

Hoyt, A. M., Gandois, L., Eri, J., Kai, F. M., Harvey, C. F., and Cobb, A. R.: CO_2 emissions from an undrained tropical peatland: Interacting influences of temperature, shading and water table depth, Global Change Biology, 25, 2885–2899, https://doi.org/10.1111/gcb.14702, 2019.

Ingram, H. A. P.: Ecohydrology of Scottish peatlands, Transactions of the Royal Society of Edinburgh: Earth Sciences, 78, 287–296, https://doi.org/10.1017/S0263593300011226, 1987.

https://doi.org/10.5194/egusphere-2024-1279
Preprint. Discussion started: 13 May 2024

Jauhiainen, J., Takahashi, H., Heikkinen, J. E. P., Martikainen, P. J., and Vasander, H.: Carbon fluxes from a tropical peat swamp forest floor, Global Change Biology, 11, 1788–1797, https://doi.org/10.1111/j.1365-2486.2005.001031.x, 2005.

Kettridge, N., Turetsky, M. R., Sherwood, J. H., Thompson, D. K., Miller, C. A., Benscoter, B. W., Flannigan, M. D., Wotton, B. M., and Waddington, J. M.: Moderate drop in water table increases peatland vulnerability to post-fire regime shift, Sci Rep, 5, 8063, https://doi.org/10.1038/srep08063, 2015.

Kotsyurbenko, O. R., Chin, K.-J., Glagolev, M. V., Stubner, S., Simankova, M. V., Nozhevnikova, A. N., and Conrad, R.: Acetoclastic and hydrogenotrophic methane production and methanogenic populations in an acidic West-Siberian peat bog, Environ Microbiol, 6, 1159–1173, https://doi.org/10.1111/j.1462-2920.2004.00634.x, 2004.

Lähteenoja, O., Reátegui, Y. R., Räsänen, M., Torres, D. D. C., Oinonen, M., and Page, S.: The large A mazonian peatland carbon sink in the subsiding P astaza- M arañón foreland basin, P eru, Global Change Biology, 18, 164–178, https://doi.org/10.1111/j.1365-2486.2011.02504.x, 2012.

Lampela, M., Jauhiainen, J., and Vasander, H.: Surface peat structure and chemistry in a tropical peat swamp forest, Plant Soil, 382, 329–347, https://doi.org/10.1007/s11104-014-2187-5, 2014.

Ledru, M.-P., Braga, P. I. S., Soubiès, F., Fournier, M., Martin, L., Suguio, K., and Turcq, B.: The last 50,000 years in the Neotropics (Southern Brazil): evolution of vegetation and climate, Palaeogeography, Palaeoclimatology, Palaeoecology, 123, 239–257, https://doi.org/10.1016/0031-0182(96)00105-8, 1996.

Li, D., Ni, H., Jiao, S., Lu, Y., Zhou, J., Sun, B., and Liang, Y.: Coexistence patterns of soil methanogens are closely tied to methane generation and community assembly in rice paddies, Microbiome, 9, 20, https://doi.org/10.1186/s40168-020-00978-8, 2021.

Liebner, S., Ganzert, L., Kiss, A., Yang, S., Wagner, D., and Svenning, M. M.: Shifts in methanogenic community composition and methane fluxes along the degradation of discontinuous permafrost, Front. Microbiol., 6, https://doi.org/10.3389/fmicb.2015.00356, 2015.

Loisel, J., Gallego-Sala, A. V., Amesbury, M. J., Magnan, G., Anshari, G., Beilman, D. W., Benavides, J. C., Blewett, J., Camill, P., Charman, D. J., Chawchai, S., Hedgpeth, A., Kleinen, T., Korhola, A., Large, D., Mansilla, C. A., Müller, J., Van Bellen, S., West, J. B., Yu, Z., Bubier, J. L., Garneau, M., Moore, T., Sannel, A. B. K., Page, S., Väliranta, M., Bechtold, M., Brovkin, V., Cole, L. E. S., Chanton, J. P., Christensen, T. R., Davies, M. A., De Vleeschouwer, F., Finkelstein, S. A., Frolking, S., Gałka, M., Gandois, L., Girkin, N., Harris, L. I., Heinemeyer, A., Hoyt, A. M., Jones, M. C., Joos, F., Juutinen, S., Kaiser, K., Lacourse, T., Lamentowicz, M., Larmola, T., Leifeld, J., Lohila, A., Milner, A. M., Minkkinen, K., Moss, P., Naafs, B. D. A., Nichols, J., O'Donnell, J., Payne, R., Philben, M., Piilo, S., Quillet, A., Ratnayake, A. S., Roland, T. P., Sjögersten, S., Sonnentag, O., Swindles, G. T., Swinnen, W., Talbot, J., Treat, C., Valach, A. C., and Wu, J.: Expert assessment of future vulnerability of the global peatland carbon sink, Nat. Clim. Chang., 11, 70–77, https://doi.org/10.1038/s41558-020-00944-0, 2021.

Malmer, N. and Holm, E.: Variation in the C/N-Quotient of Peat in Relation to Decomposition Rate and Age Determination with 210 Pb, Oikos, 43, 171, https://doi.org/10.2307/3544766, 1984.

McNicol, G., Knox, S. H., Guilderson, T. P., Baldocchi, D. D., and Silver, W. L.: Where old meets new: An ecosystem study of methanogenesis in a reflooded agricultural peatland, Global Change Biology, 26, 772–785, https://doi.org/10.1111/gcb.14916, 2020.

https://doi.org/10.5194/egusphere-2024-1279
Preprint. Discussion started: 13 May 2024

Noon, M. L., Goldstein, A., Ledezma, J. C., Roehrdanz, P. R., Cook-Patton, S. C., Spawn-Lee, S. A., Wright, T. M., Gonzalez-Roglich, M., Hole, D. G., Rockström, J., and Turner, W. R.: Mapping the irrecoverable carbon in Earth's ecosystems, Nat Sustain, 5, 37–46, https://doi.org/10.1038/s41893-021-00803-6, 2021.

Norris, M. W., Turnbull, J. C., Howarth, J. D., and Vandergoes, M. J.: Pretreatment of Terrestrial Macrofossils, Radiocarbon, 62, 349–360, https://doi.org/10.1017/RDC.2020.8, 2020.

Nottingham, A. T., Bååth, E., Reischke, S., Salinas, N., and Meir, P.: Adaptation of soil microbial growth to temperature: Using a tropical elevation gradient to predict future changes, Global Change Biology, 25, 827–838, https://doi.org/10.1111/gcb.14502, 2019.

Ofiti, N. O. E., Schmidt, M. W. I., Abiven, S., Hanson, P. J., Iversen, C. M., Wilson, R. M., Kostka, J. E., Wiesenberg, G. L. B., and Malhotra, A.: Climate warming and elevated CO2 alter peatland soil carbon sources and stability, Nat Commun, 14, 7533, https://doi.org/10.1038/s41467-023-43410-z, 2023.

Omar, M. S., Ifandi, E., Sukri, R. S., Kalaitzidis, S., Christanis, K., Lai, D. T. C., Bashir, S., and Tsikouras, B.: Peatlands in Southeast Asia: A comprehensive geological review, Earth-Science Reviews, 232, 104149, https://doi.org/10.1016/j.earscirev.2022.104149, 2022.

Osaki, M., Kato, T., Kohyama, T., Takahashi, H., Haraguchi, A., Yabe, K., Tsuji, N., Shiodera, S., Rahajoe, J. S., Atikah, T. D., Oide, A., Matsui, K., Wetadewi, R. I., and Silsigia, S.: Basic Information About Tropical Peatland Ecosystems, in: Tropical Peatland Eco-management, edited by: Osaki, M., Tsuji, N., Foead, N., and Rieley, J., Springer Singapore, Singapore, 3–62, https://doi.org/10.1007/978-981-33-4654-3_1, 2021.

Page, S. E., Rieley, J. O., and Banks, C. J.: Global and regional importance of the tropical peatland carbon pool, Global Change Biology, 17, 798–818, https://doi.org/10.1111/j.1365-2486.2010.02279.x, 2011.

Phillips, S. and Bustin, R. M.: Sedimentology of the Changuinola peat deposit: Organic and clastic sedimentary response to punctuated coastal subsidence, Geological Society of America Bulletin, 108, 794–814, https://doi.org/10.1130/0016-7606(1996)108<0794:SOTCPD>2.3.CO;2, 1996.

Phillips, S., Rouse, G. E., and Bustin, R. M.: Vegetation zones and diagnostic pollen profiles of a coastal peat swamp, Bocas del Toro, Panamá, Palaeogeography, Palaeoclimatology, Palaeoecology, 128, 301–338, https://doi.org/10.1016/S0031-0182(97)81129-7, 1997.

Ribeiro, K., Pacheco, F. S., Ferreira, J. W., De Sousa-Neto, E. R., Hastie, A., Krieger Filho, G. C., Alvalá, P. C., Forti, M. C., and Ometto, J. P.: Tropical peatlands and their contribution to the global carbon cycle and climate change, Global Change Biology, 27, 489–505, https://doi.org/10.1111/gcb.15408, 2021.

Ruwaimana, M., Anshari, G. Z., Silva, L. C. R., and Gavin, D. G.: The oldest extant tropical peatland in the world: a major carbon reservoir for at least 47 000 years, Environ. Res. Lett., 15, 114027, https://doi.org/10.1088/1748-9326/abb853, 2020.

Sihi, D., Inglett, P. W., and Inglett, K. S.: Carbon quality and nutrient status drive the temperature sensitivity of organic matter decomposition in subtropical peat soils, Biogeochemistry, 131, 103–119, https://doi.org/10.1007/s10533-016-0267-8, 2016.

Sjögersten, S., Cheesman, A. W., Lopez, O., and Turner, B. L.: Biogeochemical processes along a nutrient gradient in a tropical ombrotrophic peatland, Biogeochemistry, 104, 147–163, https://doi.org/10.1007/s10533-010-9493-7, 2011.

Sugimoto, A. and Wada, E.: Carbon isotopic composition of bacterial methane in a soil incubation experiment: Contributions of acetate and, Geochimica et Cosmochimica Acta, 57, 4015–4027, https://doi.org/10.1016/0016-7037(93)90350-6, 1993.

https://doi.org/10.5194/egusphere-2024-1279
Preprint. Discussion started: 13 May 2024

Sun, C. L., Brauer, S. L., Cadillo-Quiroz, H., Zinder, S. H., and Yavitt, J. B.: Seasonal Changes in Methanogenesis and Methanogenic Community in Three Peatlands, New York State, Front. Microbio., 3, https://doi.org/10.3389/fmicb.2012.00081, 2012.

Troxler, T. G.: Patterns of phosphorus, nitrogen and δ ^{15} N along a peat development gradient in a coastal mire, Panama, J. Trop. Ecol., 23, 683–691, https://doi.org/10.1017/S0266467407004464, 2007.

Troxler, T. G., Ikenaga, M., Scinto, L., Boyer, J. N., Condit, R., Perez, R., Gann, G. D., and Childers, D. L.: Patterns of Soil Bacteria and Canopy Community Structure Related to Tropical Peatland Development, Wetlands, 32, 769–782, https://doi.org/10.1007/s13157-012-0310-z, 2012.

United Nations Environment Programme, Global Environment Facility, Asia Pacific Network for Global Change Research, Global Environment Centre (Malaysia), and Wetlands International (Eds.): Assessment on peatlands, biodiversity, and climate change, Global Environment Centre & Wetlands International, Wageningen, Kuala Lumpur, 2 pp., 2008.

Upton, A., Vane, C. H., Girkin, N., Turner, B. L., and Sjögersten, S.: Does litter input determine carbon storage and peat organic chemistry in tropical peatlands?, Geoderma, 326, 76–87, https://doi.org/10.1016/j.geoderma.2018.03.030, 2018.

Wilson, R. M., Hopple, A. M., Tfaily, M. M., Sebestyen, S. D., Schadt, C. W., Pfeifer-Meister, L., Medvedeff, C., McFarlane, K. J., Kostka, J. E., Kolton, M., Kolka, R. K., Kluber, L. A., Keller, J. K., Guilderson, T. P., Griffiths, N. A., Chanton, J. P., Bridgham, S. D., and Hanson, P. J.: Stability of peatland carbon to rising temperatures, Nat Commun, 7, 13723, https://doi.org/10.1038/ncomms13723, 2016.

Wilson, R. M., Griffiths, N. A., Visser, A., McFarlane, K. J., Sebestyen, S. D., Oleheiser, K. C., Bosman, S., Hopple, A. M., Tfaily, M. M., Kolka, R. K., Hanson, P. J., Kostka, J. E., Bridgham, S. D., Keller, J. K., and Chanton, J. P.: Radiocarbon Analyses Quantify Peat Carbon Losses With Increasing Temperature in a Whole Ecosystem Warming Experiment, JGR Biogeosciences, 126, e2021JG006511, https://doi.org/10.1029/2021JG006511, 2021.

Wright, E. L., Black, C. R., Cheesman, A. W., Drage, T., Large, D., Turner, B. L., and Sjögersten, S.: Contribution of subsurface peat to CO2 and CH4 fluxes in a neotropical peatland: CARBON FLUXES IN A NEOTROPICAL PEATLAND, Global Change Biology, 17, 2867–2881, https://doi.org/10.1111/j.1365-2486.2011.02448.x, 2011.

Wright, E. L., Black, C. R., Turner, B. L., and Sjögersten, S.: Environmental controls of temporal and spatial variability in CO_2 and CH_4 fluxes in a neotropical peatland, Global Change Biology, 19, 3775–3789, https://doi.org/10.1111/gcb.12330, 2013.

Zhang, Y., Ma, A., Zhuang, G., and Zhuang, X.: The acetotrophic pathway dominates methane production in Zoige alpine wetland coexisting with hydrogenotrophic pathway, Sci Rep, 9, 9141, https://doi.org/10.1038/s41598-019-45590-5, 2019.